

# Clownfish metapopulation persistence draft

Allison G. Dedrick<sup>a,\*</sup>

Katrina A. Catalano<sup>a</sup>

Michelle R. Stuart<sup>a</sup>

J. Wilson White<sup>b</sup>

Humberto Montes, Jr.<sup>c</sup>

Malin Pinsky<sup>a</sup>

a. Department of Ecology Evolution and Natural Resources, Rutgers University, 14 College Farm Road, New Brunswick, NJ 08901;

b. Oregon State University

c. Visayas State University

\* Corresponding author; e-mail: agdedrick@gmail.com

*(Author order not yet determined)*

## Introduction

Metapopulations exist along a continuum, with dynamics driven by the balance of

<sup>3</sup> extinction and colonization of local patches at one extreme and focused on the bal-

ance of immigration and emmigration at constantly-occupied local patches at the other (Kritzer and Sale, 2006). Terrestrial metapopulations often show extinction-  
6 colonization dynamics (e.g. Hanski, 1998), while marine metapopulations tend to exhibit immigration-emmigration dynamics where local extinction of patches is un-  
common (Kritzer and Sale, 2006). For these marine metapopulations, dynamics  
9 and persistence depend on connectivity among patches and the demographic rates at each patch (e.g. Hastings and Botsford, 2006a; Hanski, 1998). Assessing levels of connectivity and demographic parameters has been particularly challenging for  
12 marine species, where much of the mortality and movement happens at larval and juvenile stages when individuals are hard to track and have the potential to travel long distances with ocean currents (e.g. Kritzer and Sale, 2006; Cowen and Sponaugle, 2009; Roughgarden et al., 1988). A need to understand metapopulations for  
15 conservation and management, such as siting marine protected areas (e.g. Botsford et al., 2001; White et al., 2010), however, has led to a large body of theory describing  
18 how marine metapopulations might persist.

For any population to persist, individuals must on average replace themselves during their lifetime. Assessing replacement must take into account the demographic processes across the whole life cycle, including how likely individuals are to survive to the next age or stage, their expected fecundity at each stage, and the survival of any offspring produced to recruitment. In a spatially-structured population, as many  
21 marine populations are, in addition to assessing whether the reproductive output  
24 and survival of a population is sufficient, we must also consider how the offspring are distributed across space. Marine larvae were once thought to be well-mixed and dis-

<sup>27</sup> persed far on ocean currents (e.g. Roughgarden et al., 1988), suggesting widespread connectivity among patches and largely open populations. Recent advances in estimating connectivity through natural tags and genetics, however, suggest that dispersal may be more limited (e.g. D'Aloia et al., 2013; Hameed et al., 2016; Almany et al., 2017), and local persistence of marine populations on a small spatial scale is seeming more possible.

<sup>33</sup> Considering both the demographic processes within patches and the connectivity among them, a metapopulation can persist in two ways: 1) at least one patch can achieve replacement in isolation, or 2) patches receive enough recruitment to achieve replacement through multi-generational loops of connectivity with other patches in the metapopulation (Hastings and Botsford, 2006a; Burgess et al., 2014). In the first case (termed self-persistence), enough of the reproductive output produced at one patch is retained at the patch for it to persist. In the second (network persistence), closed loops of connectivity among at least some of the patches - where individuals from one patch settle at another and eventually send offspring back to the first in a future generation - provide the patch with enough recruitment to persist within the network. Though it has been challenging to estimate the parameters necessary to understand how actual metapopulations persist, a large work of theory developed in part to guide marine protected area design helps predict when each type of persistence is likely to occur (i.e., large patches relative to the mean dispersal distance are likely to be self-persistent, Botsford et al., 2001).

<sup>48</sup> New ways of identifying individuals and determining their origins, such as otolith and shell microchemistry and genetic parentage analysis (e.g. Wang, 2004, 2014) are

making it increasingly possible to estimate both the demographic (e.g. Carson et al.,  
51 Hameed et al., 2016) and the dispersal (e.g. Almany et al., 2017; D'Aloia et al.,  
2013) parameters necessary to assess persistence in real metapopulations. We might  
expect that populations on isolated islands are the most likely to be self-persistent,  
54 as they lack nearby populations with which to exchange larvae and would go locally  
extinct if they did not achieve replacement. At isolated Kimbe Island in Papua New  
Guinea, Salles et al. (2015) find that the population of orange clownfish (*Amphiprion*  
57 *percula*) can likely persist without outside immigration. In contrast, populations of  
bicolor damselfish (*Stegastes partitus*) at a set of reef patches across four isolated  
islands in the Bahamas do not appear able to persist without outside input (Johnson  
60 et al., 2018). For populations that exist in patches along a continuous linear coastline,  
rather than on separate islands, however, how patches interact and what the scale  
of metapopulation persistence is are still open questions.

63 The number of studies estimating demographic rates and connectivity in marine  
metapopulations is growing (e.g. Salles et al., 2015; Johnson et al., 2018; Garavelli  
et al., 2018), but most use data from one or a few years. Longer data sets enable  
66 better estimates of long-term average rates, rather than assuming the demographic  
and dispersal rates from a particular year or two are representative through time.  
More data is also useful for explicitly considering uncertainty, both to assess how well  
69 we understand persistence for a population and to see which parameters contribute  
most to our uncertainty. Finally, sampling over many years provides the possibility  
of comparing abundance trends to persistence metrics to see if they tell a consistent  
72 story.

Here, we further our understanding of metapopulation dynamics in a network of patches along a coastline through a study of yellowtail clownfish (*Amphiprion clarkii*) in the Philippines. We assess persistence for all patches of habitat within a 30 km stretch of coastline, which exceeds estimates of the dispersal spread for this species (Pinsky et al., 2010), suggesting the network is likely to operate as a contained metapopulation. With seven years of annual sampling data, we are able to estimate persistence metrics and replacement over the longer term and investigate abundance through time to compare with the replacement-based persistence metrics. We use our long-term data set from habitat patches on a continuous section of coastline to understand persistence within a local network.

## Methods

### **84 Persistence theory and metrics**

For a population to persist, individuals must be able to replace themselves on average at low abundance (e.g. Hastings and Botsford, 2006a; Botsford et al., 2009). In 87 non-spatially structured populations, we use criteria such as the average number of recruiting offspring each individual produces during its life (called  $R_0$  when the population is age-structured and density-independent) or the growth rate of the 90 population (such as the dominant eigenvalue  $\lambda$  of an age-structured Leslie matrix) (Caswell, 2001; Burgess et al., 2014). For spatially-structured populations, we must also consider the spatial spread of offspring, often represented through a dispersal 93 kernel or connectivity matrix (e.g. Cowen, 2006; Buston et al., 2011; Hogan et al.,

2011; DALoia et al., 2015)).

We consider three primary metrics to assess whether and how the population is  
96 persistent: 1) lifetime recruit production (LRP), to assess whether the population  
has enough surviving offspring to achieve replacement 2) self-persistence (SP), to  
assess whether any individual patch can persist in isolation without input from other  
99 patches, and 3) network persistence (NP), to assess whether the metapopulation is  
persistent as a connected unit. We explain each metric below in detail. To represent  
the uncertainty in our estimates, we calculate each metric 1000 times, pulling each  
102 input parameter from a distribution or range. In our results, we show the range of  
values of each persistence metric as well as our best estimate.

### Lifetime production of recruits

105 We find the estimated number of recruits an individual recruit will produce (lifetime  
recruit production: LRP) by multiplying the total number of eggs a recruit-sized  
individual will produce in its lifetime (lifetime egg production: LEP) by the fraction  
108 of those eggs that will survive to become recruits (egg-recruit survival:  $S_e$ ) (Fig. 2  
Metrics):

$$\text{LRP} = \text{LEP} * S_e. \quad (1)$$

If  $\text{LRP} \geq 1$ , the population has the possibility for replacement; individuals produce  
111 enough surviving offspring, before taking into account the probability of dispersal.  
If  $\text{LRP} < 1$ , the individuals are not replacing themselves and the population cannot  
persist without input from outside patches. We consider LRP for all recruits pro-

<sub>114</sub> duced by our individuals, regardless of where they settle, which requires combination  
 with the dispersal kernel to understand persistence, and for recruits that settle only  
 at our sites,  $LRP_{local}$ , which implicitly includes dispersal. If  $LRP_{local} \geq 1$ , our group  
<sub>117</sub> of sites is able to persist locally.

### Self-persistence

A patch is able to persist in isolation (self-persistent) if individuals produce enough  
<sub>120</sub> offspring that survive to recruitment ( $LRP$ ) and disperse back to the natal patch  
 (with probability of dispersal  $p_{i,i}$ ) to replace themselves. Burgess et al. (2014) use  
 LEP to represent offspring produced and local retention (LR) - the number of surviv-  
<sub>123</sub> ing recruits that disperse back to the natal patch over the number of eggs produced by  
 the natal patch - to capture egg-recruit survival and dispersal combined in a criteria  
 for self-persistence:  $LEP \times LR \geq 1$ . We modify this to include egg-recruit survival in  
<sub>126</sub> the offspring term, using  $LRP$  in place of  $LEP$ , to assess whether a particular patch  
 $i$  is self-persistent:

$$SP_i = LEP \times \frac{\text{recruits}}{\text{egg}} \times \frac{p_{i,i} \times \# \text{ recruits from patch } i}{\frac{\text{recruits}}{\text{egg}} \times \# \text{ eggs produced by patch } i} \quad (2)$$

$$SP_i = LRP \times p_{i,i}.$$

A patch is self-persistent if  $SP \geq 1$ . If at least one patch is self-persistent, the  
<sub>129</sub> metapopulation as a whole is persistent as well (Hastings and Botsford, 2006a;  
 Burgess et al., 2014).

## Realized connectivity matrix and network persistence

<sup>132</sup> We find the probabilities of a recruit dispersing between each set of sites ( $p_{i,j}$ ) by integrating the dispersal kernel (eqn. 3) over the distances between sites. We then create a realized connectivity matrix  $C$  by multiplying the dispersal probabilities by <sup>135</sup> the expected number of recruits an individual produces:  $C_{i,j} = \text{LRP} \times p_{i,j}$  (Burgess et al., 2014, though we include egg-recruit survival in LRP, rather than in  $p_{i,j}$  as they do). The diagonal entries of  $C$ , where the origin and destination are the same site, <sup>138</sup> are the values of self-persistence we calculate above.

<sup>141</sup> Network persistence requires that the largest real eigenvalue of the realized connectivity matrix  $\lambda_C$  be greater than 1:  $\text{NP} = \lambda_C > 1$  (e.g. Hastings and Botsford, 2006a; White et al., 2010; Burgess et al., 2014).

## Defining recruit and census stage

<sup>144</sup> When assessing persistence, it is important to consider mortality and reproduction that occurs across the entire life cycle to determine whether an individual is replacing itself with an individual that reaches the same life stage (Burgess et al., 2014). We define a recruit to be a juvenile individual that has settled on the reef within the <sup>147</sup> previous year, which also encompasses the size we are first able to sample (3.5-6.0 cm for parentage studies) (Fig. 2, Life stage). In theory, it does not matter how we define recruit as long as we use that definition in our calculations of both egg-recruit <sup>150</sup> survival and LEP. In our system, however, while it is straightforward to calculate LEP from any size, we do not have enough tagged recruits to reliably estimate survival

to different recruit sizes. Instead, we choose the mean size of offspring matched in  
153 the parentage study as our best estimate of the size of a recruit ( $\text{size}_{\text{recruit}}$ ) and test sensitivity to different recruit sizes by pulling from a uniform distribution over the sizes the recruit stage covers (3.5-6 cm, Table A1).

156 **Study system**

We focus on a tropical metapopulation of yellowtail clownfish (*Ampiprion clarkii*, Fig. 3c) on the west coast of Leyte island facing the Camotes Sea in the Philippines (Fig. 159 3a). Like many clownfish species, yellowtail clownfish have a mutualistic relationship with anemones, where small colonies of fish live (Buston, 2003b; Fautin et al., 1992). Yellowtail clownfish are protandrous hermaphrodites and maintain a size-structured hierarchy; within an anemone, the largest fish is the breeding female, the next largest is the breeding male, and any smaller fish are non-breeding juveniles. The fish on 162 an anemone maintain a strict social and size hierarchy (Buston, 2003b), with fish moving up in rank to become breeders only after the larger fish have died. In the tropical patch reef habitat of the Philippines, yellowtail clownfish spawn once per 165 lunar month from November to May, laying clutches of benthic eggs that the parents protect and tend (Ochi, 1989; Holtswarth et al., 2017). Larvae hatch after about six days and spend 7-10 days in the water column before returning to reef habitat to settle in an anemone (Fautin et al., 1992).

171 Clownfish are particularly well-suited to metapopulation studies due to their limited movement as adults and clearly patchy habitat. Once fish have settled, they tend to stay within close proximity of their anemones (XX meters, Stuart et al., in

<sup>174</sup> prep). This makes fish easier to relocate for mark-recapture studies and simplifies  
the exchange between patches to only the dispersal during the larval phase. Patches,  
whether considered to be the reef patch or the anemone territory of the fish, are  
<sup>177</sup> clearly discrete and easily delineated (Fig. 3a, b), which makes determining the spa-  
tial structure of the metapopulation clear. Additionally, clear patches make it easier  
to assess how much of the site has been surveyed. These simplifying characteristics in  
<sup>180</sup> habitat and fish behavior make clownfish and other similarly territory-based reef fish  
useful model systems for studies of metapopulation dynamics and persistence (e.g.  
Buston and DAloia, 2013; Salles et al., 2015; Johnson et al., 2018). Our focal species  
<sup>183</sup> of yellowtail clownfish tends to behave more like larger reef fishes, with territories  
that can extend beyond single anemones (Hattori and Yanagisawa, 1991; Ochi, 1989)  
and strong enough swimming skills that movement between patch reefs is possible  
<sup>186</sup> though unusual (seen XX times at our sites, Stuart et al., in prep), than the smaller  
clownfish *A. percula* commonly used in previous metapopulation studies (e.g. Buston  
et al., 2011; Salles et al., 2015).

<sup>189</sup> **Field data collection**

We focus on a set of seventeen patch reef sites spanning approximately 30 km along  
the western coast of Leyte island (Fig. 3a). The sites consist of rocky patches of coral  
<sup>192</sup> reef and are separated by sand flats (Fig. 3b). Previous work using genetic isolation  
by distance estimated that yellowtail clownfish larvae have a dispersal spread of about  
10 km (range 4-27 km, Pinsky et al., 2010), so our sites were selected to cover and  
<sup>195</sup> exceed that range. On the north edge, the sites are isolated from nearby habitat

with no substantial reef habitat for at least 20 km.

Since 2012, we have sampled fish and habitat at most of the sites annually (Table 198 A2). During sampling, divers using SCUBA and tethered to GPS readers swam the extent of each site. Divers visited each anemone inhabited by yellowtail clownfish, tagging the anemone to track it through time. At each anemone, the divers attempted 201 to catch all of the yellowtail clownfish 3.5 cm and larger, taking a small tail fin-clip from each for use in genetic analysis, measuring the fork length, and noting the tail color (as an indicator of life stage). Starting in the 2015 field season, fish 6.0 cm 204 and larger were also tagged with a passive integrated transponder (PIT) tag, unless already tagged. Divers also looked for eggs around each anemone and measured and photographed any clutches found. In total, we took fin clips from and genotyped 207 2772 fish and PIT-tagged 1929 fish across all years and sites combined, marking 3413 individual fish.

### Parentage analysis and dispersal kernel

210 We genotyped 2772 fish from our tissue samples and used single nucleotide polymorphisms to identify parent-offspring matches with the software program COLONY2 213 (Wang, 2012) (details on genotyping and parentage analysis in Catalano et al., in prep).

Using the method described in (Bode et al., 2018), we fit a distance-based dispersal kernel (Catalano et al., in prep), where the relative dispersal is a function of 216 distance  $d$  as measured in kilometers and parameters  $\theta$  and  $z = e^{kd}$ , which control

the shape and scale of the kernel:

$$p(d) = ze^{-(zd)^\theta}. \quad (3)$$

We use a Laplacian dispersal kernel with shape parameters  $\theta = 1$  and scale parameter  $k_d = -2.11$  (Fig. 4a, estimated in (Catalano et al., in prep)). To account for uncertainty in the dispersal kernel, we keep the shape parameter  $\theta$  constant and pull the scale parameter  $k_d$  from a set capturing the 95% interval produced during kernel estimation in Catalano et al. (in prep).

The dispersal kernel is estimated using fish that have already recruited to a population and survived to be sampled so it gives the relative amount of dispersal given that a fish recruits somewhere, not the probability that a released larva will travel a particular distance. To find the probability of fish dispersing among our sites, we numerically integrate the dispersal kernel (eqn. 3) using the distance from the middle of the origin site to the closest and farthest bounds of the destination site as the upper and lower bounds. For example, the probability of dispersal from site A to B, where  $d_1$  is the distance from the middle of A to the closest edge of B and  $d_2$  is the distance from the middle of A to the far edge of B, is:

$$p_{A,B}(d) = \int_{d_1}^{d_2} ze^{-(zd)^\theta} dd. \quad (4)$$

## Estimating inputs from empirical data

### Growth and survival: mark-recapture analyses

- <sup>234</sup> We mark fish through both genetic samples and PIT tags, allowing us to estimate growth and survival through mark-recapture. After matching up recaptures of the same fish identified by genotype or tag, we have a set of encounters of 3413 marked fish that includes size and stage at each capture time.
- <sup>237</sup>

For growth, we estimate the parameters of a von Bertalanffy growth curve (Fabens, 1965) in the growth increment form relating the length at first capture  $L_t$  to the length at a later capture  $L_{t+1}$  (Hart and Chute, 2009), where  $L_\infty$  is the average asymptotic size across the population and  $K$  controls the rate of growth:

<sup>240</sup>

$$\begin{aligned} L_{t+1} &= L_t + (L_\infty - L_t)[1 - e^{(-K)}] \\ &= e^{(-K)}L_t + L_\infty[1 - e^{(-K)}]. \end{aligned} \tag{5}$$

We see from eqn. 5 that we would expect the first length  $L_t$  and the second length  $L_{t+1}$  to be related linearly (Hart and Chute, 2009). From the slope  $m = e^{(-K)}$  and y-intercept  $b = L_\infty[1 - e^{(-K)}]$ , we can estimate the von Bertalanffy parameters, such that  $K = -\ln m$  and  $L_\infty = \frac{b}{(1-m)}$ . We use the first and second capture lengths for fish that were recaptured after a year (within 345 to 385 days) to estimate  $L_\infty$  and  $K$ .

<sup>243</sup>

We have some fish that were recaptured multiple times so we randomly select only one pair of recaptures from each to use in estimating the parameters, then repeat

<sup>246</sup>

249 this process 1000 times to generate a distribution.

We use the full set of marked fish to estimate annual survival  $\phi$  and probability of recapture  $p_r$  using the mark-recapture program MARK implemented in R (Laake, 252 2013). We consider several models with year, size, and site effects on the probability of survival on a log-odds scale (see full list in Table A3). For fish that are not recaptured in particular year, we estimate their size using our growth model (eqn. 255 5) and the size recorded or estimated in the previous year. Because fish are not well-mixed at our sites and instead stay quite close to their home anemones, we need to swim near an anemone to have a reasonable chance of capturing the fish on it. 258 Therefore, we also consider a distance effect on recapture probability; we use the GPS tracks of divers to estimate the minimum distance between a diver and the anemone for each tagged fish in each sample year and include it as a factor in some 261 of the models (Table A3).

## Fecundity

We use a size-dependent fecundity relationship, determined using photos of egg 264 clutches and females (Yawdoszyn, in prep), where the number of eggs per clutch ( $E_c$ ) is exponentially related to the length in cm of the female ( $L$ ) with size effect  $\beta_l = 2.388$ , intercept  $b = 1.174$ , and egg age effect  $\beta_e = -0.6083$  dependent on if the 267 eggs are old enough to have visible eyes:

$$\ln(E_c) = \beta_l \ln(L) + \beta_e[\text{eyed}] + b. \quad (6)$$

To get total annual fecundity  $f$ , we multiply the number of eyed eggs per clutch by the number of clutches per year  $c_e = 11.9$ , using the estimate from Holtswarth et al.  
270 (2017).

We only consider reproductive effort once the fish has reached the female stage and use the average size of first observation as female for recaptured fish as the  
273 transition size  $L_f = 9.32\text{cm}$ . To incorporate uncertainty, we draw from the full set of sizes at which recaptured fish were first captured as female (5.2 cm - 12.7 cm).

### Lifetime egg production

276 We use an integral projection model (IPM) (e.g. Rees et al., 2014) with size as the continuous structuring trait  $z$  to estimate lifetime egg production (LEP), the total number of eggs produced by one individual, starting at the recruit stage. We initialize  
279 the IPM with one recruit-sized individual ( $\text{size}_{\text{recruit}}$ ) at the initial time step ( $t = 0$ ), then project forward for 100 time steps using the size-dependent survival (eqn. 11) and growth (eqn. 5) functions as the probability density functions that make up the  
282 kernel to describe the survival and growth of the individual into the next time step. This gives us the size distribution at each time step, which represents the probability that the individual has survived and grown into each of the possible size categories,  
285 ranging from a minimum of  $L = 0\text{ cm}$  to a maximum of  $U = 15\text{ cm}$ . The probability that the individual is still alive and of any size decreases as the time steps progress; by using a large number of steps, we are able to avoid arbitrarily setting a maximum  
288 age and instead let the probabilities become essentially zero.

We then multiply the size-distribution  $v_z$  at each time by the size-dependent

fecundity  $f_z$  described above (eqn. 6) to get the total number of eggs produced at  
<sup>291</sup> each time step. We then integrate across time and size to get the total number of eggs one individual is likely to produce in its lifetime:

$$\text{LEP} = \int_{t=0}^{100} \int_{z=L}^{z=U} v_{z,t} f_z dz dt. \quad (7)$$

To compute LEP, we discretize time and size and sum across the matrix. We  
<sup>294</sup> use 0.1 as the standard deviation of size for a recruit ( $\text{size}_{\text{recruit},sd}$ ) and estimate the standard deviation of the distribution of sizes of fish in the next year ( $\text{size}_{sd}$ ) from our recapture data (A1).

#### <sup>297</sup> Survival from egg to recruit

We estimate survival from egg to recruit ( $S_e$ ) using parentage matches to estimate the number of surviving recruits produced by genotyped parents (similar to the  
<sup>300</sup> method in Johnson et al., 2018). We scale the number of offspring we match back to parents ( $R_m = 62$ ) by various ways we could have missed offspring ( $P_h$ ,  $P_c$ ,  $P_d$ , and  $P_s$ , described below), then divide by the estimated number of eggs produced by  
<sup>303</sup> genotyped parents, found by multiplying the number of genotyped parents ( $N_g = 1719$ ) by the expected lifetime egg production for a fish of parent size (LEP<sub>p</sub>):

$$S_e = \frac{\frac{R_m}{P_h P_c P_d P_s}}{N_g \text{LEP}_p}. \quad (8)$$

We scale the number of matched recruits we find by the cumulative proportion of  
<sup>306</sup> habitat in our sites we sampled over time ( $P_h = 0.41$ , details in A.1), the probability

of capturing a fish if we sampled its anemone ( $P_c = 0.56$ , see A.2 for details), and the proportion of the total dispersal kernel area from each our of sites covered within  
309 our sampling region ( $P_d = 0.57$ , calculation in A.2). Finally, because our dispersal kernel gives the probability of dispersal given that a recruit settled somewhere but our sampling region is not all habitat, we scale by the proportion habitat in our  
312 sampling region ( $P_s = 0.20$ , details in A.3) to avoid counting this mortality twice.

To estimate  $\text{LRP}_{\text{local}}$ , we scale only by the proportion of habitat we cumulatively sample in our sites and the probability of capturing a fish.

315 To incorporate uncertainty in our estimate of egg-recruit survival, we consider uncertainty in the number of offspring assigned to parents during the parentage analysis ( $R_m$ ) and in the probability of capturing a fish ( $P_c$ ). We generate a set  
318 of values for the number of assigned offspring using a random binomial, where the number of trials is the number of genotyped offspring (745) and the probability of success on each trial is the assignment rate of offspring from the parentage analysis  
321 (0.079) (Catalano et al., in prep). For the probability of capturing a fish, we pull values from a beta distribution that captures the mean and variance of capture probabilities across recapture dives (details in A.2).

### 324 Accounting for density-dependence

Ideally we would assess persistence metrics when the population is at low abundance and not limited by density-dependence. Clownfish have strong social hierarchies and  
327 juveniles on an anemone will prevent others from settling there as well (seen in *A. percula*, Buston, 2003a). Each anenome, therefore, can only house one settling clown-

fish, with anemones already occupied by *A. clarkii* settlers essentially unavailable as  
 330 habitat. We attempt to account for this density-dependent mortality by multiplying-  
 ing our estimate of settling recruits (the numerator of eqn. 8) by the proportional  
 increase (DD) in unoccupied anemones at our sites if all of the *A. clarkii* anemones  
 333 were unoccupied, where  $p_A$  is the proportion of anemones occupied by *A. clarkii* and  
 $p_U$  is the proportion of unoccupied anemones:  $DD = \frac{(p_U + p_A)}{p_U}$ . We present results  
 both with and without this density-dependence modification.

### 336 Estimated abundance over time

We also consider trends in abundance of breeding females at each site over time to  
 compare to our replacement-based estimates of persistence. Similarly to as we do for  
 339 offspring, we scale up the number of females caught at each site  $i$  in each sampling  
 year  $t$  by the proportion of habitat sampled in that site and year  $P_{h_{i,t}}$  and by the  
 probability of capturing a fish  $P_c$ :

$$\# \text{ females}_{i,t} = \frac{\# \text{ females captured}_{i,t}}{P_{h_{i,t}} P_c}. \quad (9)$$

342 We then fit a linear model through the time series for each site  $i$  sampled in at  
 least three years to assess whether the slope over time is positive or negative:

$$\# \text{ females}_i \sim \text{year} \quad (10)$$

## Results

<sup>345</sup> Our estimated abundance of females at each site over time does not suggest a clear trend (Fig. 1). In our very simple look at whether abundance seems to be increasing or decreasing, eleven sites had a positive slope over time and five had a negative slope (<sup>348</sup> Fig. 1q). For the two largest sites, with a mean estimated number of females of between 150-200, one has a positive slope (Wangag, Fig. 1b) and one has a negative slope (Sitio Baybayon, Fig. 1p) and the next two largest sites are also split (Palanas, Fig. 1a and Haina, Fig. 1o). Overall, there is not a clear directional change in abundance across the sites we sample over our sampling period.

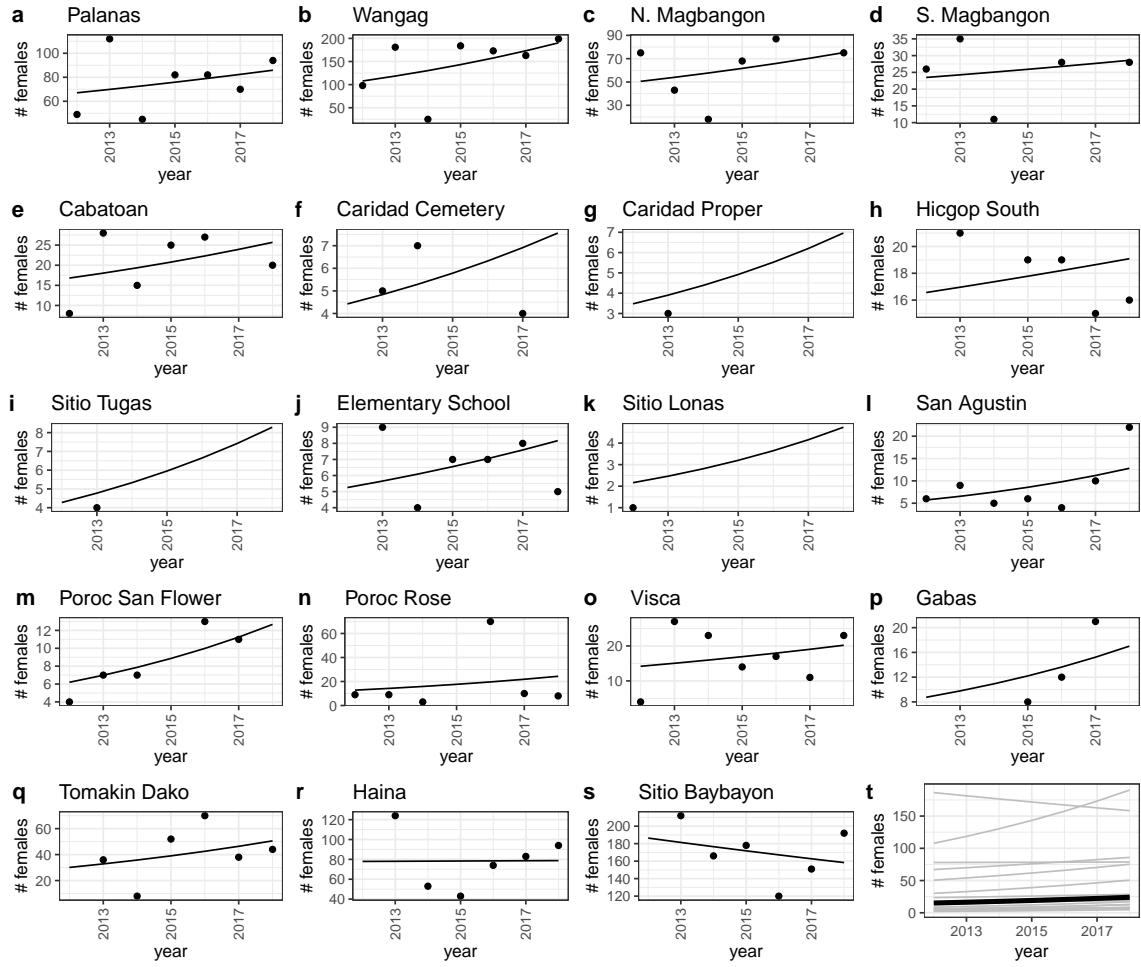


Figure 1: The estimated number of females at each site over the sampling years for sites sampled in at least three years. The total number of females at each site was estimated by scaling up the number of females captured at each site in each year by the proportion of habitat sampled at that site that season (see A.1 for details) and by the average probability of capturing a fish (see A.2). We show the estimated abundances and trend for each site individually (a-p) and a histogram of the slopes of abundance through time (q).

From the mark-recapture analysis of tagged and genotyped fish, we estimate mean values of  $L_\infty = 10.71\text{cm}$  (range of estimates 10.50 - 10.90 cm) and  $K = 0.864$  (range

354

of estimates 0.785 - 0.944) for the von Bertalanffy growth curve parameters (eqn. 5, Fig. 4b, Table A1). For juvenile and adult (post-recruitment) survival on a log-odds scale, the best-fit model has an effect of size, with coefficient  $b_a = 0.169 \pm 0.028$  SE and intercept  $b_\phi = -1.83 \pm 0.231$  SE (eqn. 11). The accompanying best-fit model for log-odds recapture probability has a negative size effect and a negative effect of diver distance from the anemone (eqn. A.3, Fig. A.3).

$$\log\left(\frac{\phi}{1-\phi}\right) = b_\phi + b_a \text{size.} \quad (11)$$

Using our best estimates for growth, survival, and fecundity, we calculate a value for LEP of 1061, ranging from 39 to 10345 when we consider uncertainty in the inputs (Fig. 5b). Adult survival has the most effect on the value of LEP (Fig. B.4), with higher values of LEP the higher annual survival of adults.

We estimate egg-recruit survival  $S_e$  to be 7.8e-04, ranging from 1.2e-04 to 0.033 when we include uncertainty in the number of offspring assigned to parents and the probability of catching a fish (APPENDIX FIG!). When we compensate for density-dependence in our data, we estimate  $S_e$  to be 0.0013, ranging from 2.1e-04 to 0.057. These are somewhat high values of egg-recruit survival compared to what we see elsewhere in the literature (e.g. Rumrill, 1990; Metaxas and Saunders, 2009) (though not unreasonable, e.g. White et al., 2014; Johnson et al., 2018) because we scale up by the amount of habitat in our sampling area and count mortality due to dispersal to non-habitat in the dispersal probability, rather than in  $S_e$ . Uncertainty in the size of transition to breeding female  $L_f$  has the largest effect on egg-recruit survival (Fig.

<sup>375</sup> B.7); we only consider reproduction from females, to avoid double-counting, so the larger the transition size to female, the fewer tagged eggs we estimate were produced by genotyped parents and the higher egg-recruit survival.

<sup>378</sup> We estimate lifetime recruit production (LRP), the product of LEP and  $S_e$ , to be 0.83, with a range of 0.28 - 3.89 when we consider uncertainty in inputs. When we compensate for density-dependence, we estimate a value of 1.42 for LRP, with a <sup>381</sup> range of 0.48 - 6.66. The value when we compensate for density-dependence and the range of uncertainty for both are above the threshold of one necessary for replacement before considering dispersal. This mean that individuals at our sites produce enough <sup>384</sup> surviving offspring before considering dispersal to be able to replace themselves, but LRP does not tell us whether those offspring will settle within our sample sites and drive persistence.

<sup>387</sup> We also estimate replacement for recruits from our sites returning to our sites,  $LRP_{local}$ , which implicitly includes dispersal mortality, to be 0.09 (ranging from 0.03 to 0.44 when we include uncertainty) or 0.16 (0.05 to 0.76) when we compensate for <sup>390</sup> density-dependence. With a value well below one, this suggests individuals at our sites do not replace themselves with recruits that settle in our sites, suggesting our sites do not persist as an independent network. When we calculate  $LRP_{local}$  using all <sup>393</sup> arriving recruits to our sites, however, rather than just those originating there, the best estimates are  $> 1$  whether or not we compensate for density dependence (2.06, 1.22, respectively), suggesting that there is recruit-recruit replacement at our sites <sup>396</sup> when we include immigrant recruits.

We do not find any sites with  $SP > 1$ , whether we compensate for density-

dependence or not (Fig. 6a), indicating that no site could persist in isolation. Given  
399 that our best estimate of LRP does not suggest replacement and only a fraction  
of those offspring stay at the natal site, this makes sense. We see the highest val-  
ues of self-persistence at Haina (SP = 0.079, 0.13 when compensating for density-  
402 dependence) and Wangag (SP = 0.048, 0.082 when compensating for density-dependence),  
our two widest sites.

For network persistence, our best estimate of the dominant eigenvalue of the  
405 realized connectivity matrix  $\lambda_c$  is 0.21 with a range of 0.07 - 0.92 (Fig. 6), or 0.36  
with a range 0.12 - 1.58 when we compensate for density-dependence (Fig. 6). Our  
sites are likely not network persistent, as our best estimates and most of the values we  
408 see in our runs with uncertainty are below one, but network persistence is possible, as  
our range of estimates does exceed one when we compensate for density-dependence.  
We see that most of the connectivity occurs among the sites in the northern part of  
411 our sample area, from Palanas to Caridad Cemetery, and at the southern part of our  
sample area from Tomakin Dako to Sitio Baybayon (Fig. 6b, d), where the largest  
sites are.

414 Based on our estimates of LRP,  $LRP_{local}$ , SP, and NP, it is possible but not likely  
that our set of sites is able to persist in isolation as a closed system. With our  
site configuration and dispersal kernel estimate, we would need a value of LRP of  
417 3.99 (an egg-recruit survival of 0.0038 with our estimated value of LEP or a value  
of LEP of 5095 or 2975 with our estimated egg-recruit survival compensating and  
not compensating for density-dependence, respectively), to have a best estimate of  
420  $\lambda_c = 1$  and network persistence.

## Discussion

We do not see strong evidence for persistence in our metric estimates. We see no  
423 evidence for self-persistence where an individual site could persist alone and weak  
evidence for network persistence; it is possible at the upper end of our range of esti-  
mates with uncertainty but not suggested by most of the range or our best estimates  
426 (Fig. 6). The abundances through time at our sites do not show a clear directional  
change, however, suggesting that the population at our sites is relatively constant  
but relies on input of recruits from outside sites to persist. The portion of coastline  
429 we sampled is likely a sink portion of a larger metapopulation.

For our sites to be able to persist as a network on their own, the number of  
surviving recruits produced by an average recruit - LRP - would likely need to be  
432 higher. With our estimated connectivity, LRP would need to be at least 3.99 to  
see network persistence among our sites, which is within the top of our range of  
uncertainty but about 3-5 times higher than our best estimates, without and with  
435 density-dependence compensation. Our best estimate of LRP when we com-  
pensate for density-dependence is greater than one, so higher connectivity and retention  
of offspring among our sites could lead to network persistence, but almost all sur-  
438 viving offspring would need to be retained. At our best estimate without density-  
dependence compensation, however, LRP is less than one - the average recruit only  
produces 0.83 of a surviving recruit of the same stage - so no amount of increased  
441 retention or connectivity, even retaining all of the recruits produced from our sites,  
would lead to network persistence. Similarly, if other surrounding patch populations

had a similar LRP, increasing the area of the network to include them would also not  
444 achieve network persistence. If nearby sites have higher egg production or survival to  
recruit, however, it might not take much of an increase in area considered to create  
a persistence network. Nearby reef sites such as Cuatro Islas have higher quality  
447 habitat and could be contributing recruits to our sites.

We do not find clear evidence for network persistence for our sites despite esti-  
mates of the mean dispersal distance of *A. clarkii* from previous genetic work (11  
450 km, Pinsky et al., 2010) and from our samples (8.25 km, with 95% confidence in-  
terval 7.41 to 9.36, Catalano et al., in prep) that are well within the 30 km span of  
our sites. Though the width of our sampling region is more than twice the mean  
453 dispersal distance, which Lockwood et al. (2002) find sufficient for persistence of an  
isolated reserve, their estimate assumes continuous habitat within the reserve and  
our region is only about 20% habitat. For a habitat configuration more similar to  
456 our system, habitat patches (reserves) spaced on a coastline with non-habitat in be-  
tween, they find that either 40% of the coastline needs to be preserved or a minimum  
patch size must be 1.25 times the mean dispersal distance to ensure persistence. Our  
459 largest site, Haina, is only about 0.8 km wide, about 10 times less than the mean  
dispersal distance, so it is possible we do not have enough habitat in our region for  
network persistence, exacerbated by our 4 largest sites being at the edges of our  
462 area and sending half of their recruits away from our sites. Our low, and possibly  
below-replacement, estimate for LRP also suggests that lack of persistence in these  
sites is not due to excessive dispersal out of the area but due to low production and  
465 survival of offspring. The reef health and habitat quality in our sites is generally

low, due anthropogenic effects such as pollution and silt from a nearby gravel mine, and habitat disturbance due to storms. Our sites are in an area that was hit in 2013  
468 by Typhoon Haiyan, one of the strongest typhoons ever to make landfall, which de-  
stroyed much of the reef habitat in some of our northern sampling areas. This recent  
disturbance and generally low habitat quality could contribute to low production of  
471 surviving recruits in our sites (seen in other populations with low habitat quality,  
e.g. Hayashi et al., 2019) necessitating subsidization by outside populations.

We see considerable uncertainty in our estimate of persistence metrics depending  
474 on the particular input values we use (Figs. 5, B.9). Our highest estimate for LRP is  
about 24 times more than our lowest estimate and our highest NP estimate is about  
22 larger than our lowest, spanning the range between network persistence for our set  
477 of sites to far from it. Measuring demographic and dispersal parameters in the field  
is challenging; in the face of limited and imperfect data, characterizing uncertainty  
and propagating it from our estimates of demographic and dispersal inputs through  
480 to our estimates of persistence metrics is important to contextualize our results. In  
our study, uncertainty in egg-recruit survival (a commonly challenging parameter  
to estimate, e.g. Johnson et al., 2018; Hameed et al., 2016), partially driven by  
483 uncertainty in how likely we are to capture recruits during sampling (Figs. B.7,  
B.8), has a large effect on whether or not we think our populations are persistent.  
For a marine metapopulation, our system is relatively uncomplicated and yet still  
486 hard in which to concretely ascertain persistence. As we accumulate more empirical  
assessments of metapopulations to compare to our expectations from theory and  
models, we will have to think carefully about how to handle uncertainty as we move

<sup>489</sup> to tackling larger and more complicated systems.

Persistence criteria, such as those detailed in Hastings and Botsford (2006a) and Burgess et al. (2014), ask whether a population at low abundance can grow and recover rather than going extinct. Density-dependence is often ignored at low abundances (e.g. Caswell, 2001; Hastings and Botsford, 2006b) so is not explicitly considered in persistence metrics. In real populations, however, it can be challenging to estimate density-independent demographic rates, as density-dependence is occurring in the population as it is sampled. In *A. clarkii*, density-dependence is likely most important in early life stages, as for many fish species, but could play an important role throughout the life history due to the social hierarchies in colonies of clownfish (e.g. Buston and Elith, 2011). In other species of clownfish, individuals on the same anemone maintain strict size spacing, restricting their food intake and growth to avoid encroaching on the position of another fish and being attacked or evicted (seen in *A. percula*, Buston, 2003a,b). This suggests that while fish are in the pre-reproductive queue, density-dependence may lower growth rates compared to the growth of fish alone on an anemone, as would be the case in a population at low abundance. We attempt to account for the primary effect of density-dependence on our estimate of egg-recruit survival but other estimates, particularly growth and survival, would also likely be higher in the absence of density-dependence and increase LRP.

Our estimates of persistence metrics suggest that it is possible but not likely that the region of sites we sample persist as a network without outside input, despite covering an area more than twice the estimated mean dispersal distance for our focal

species. Our estimate of LRP near the threshold of one required for replacement  
513 (slightly  $< 1$  when we do not compensate for density-dependence, slightly  $> 1$  when  
we do), suggests that dispersal is not likely the primary reason our sites do not persist  
as a network. If density-dependence is strongly present in our data such that our  
516 compensated estimate is the best, then our sites could persist if there were no losses  
to dispersal. Otherwise, our sites do not produce enough offspring for replacement  
regardless of dispersal patterns, possibly due to worsening habitat quality. This is  
519 a reminder that dispersal is only part of the persistence story for metapopulations;  
even areas that seem large enough to contain a persistent network based on dispersal  
distance will not be able to persist in isolation if they have low production and  
522 survival of offspring. We do find recruits coming back to our region, and even to  
their natal site, but broader connectivity to more productive sites likely enables our  
sites to persist.

525 **Figures**

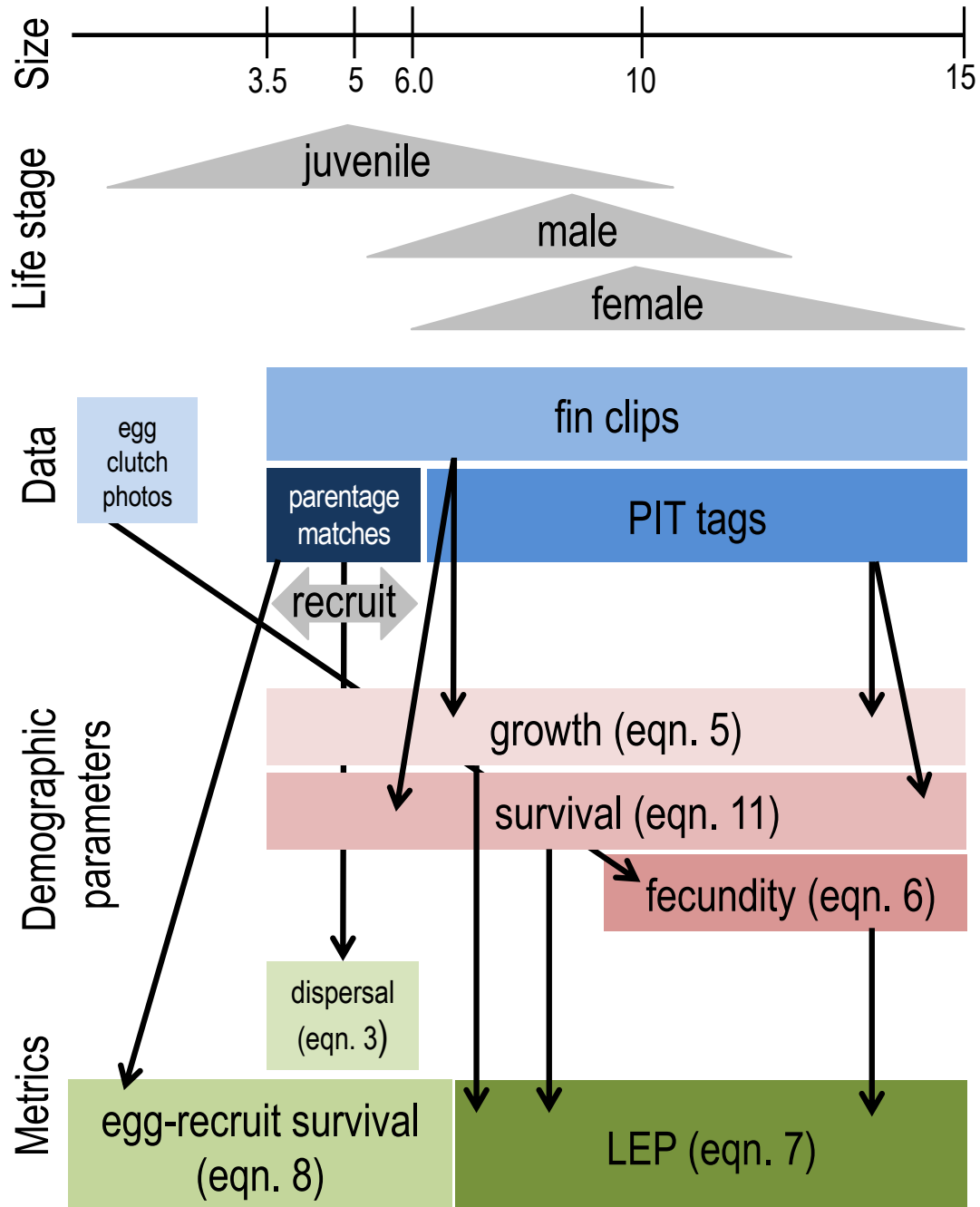


Figure 2: Here, we show the data collected<sup>29</sup> for fish at each life stage (life stage boxes are not scaled by length of stage) and how the empirical data fit into our parameter and metric calculations.

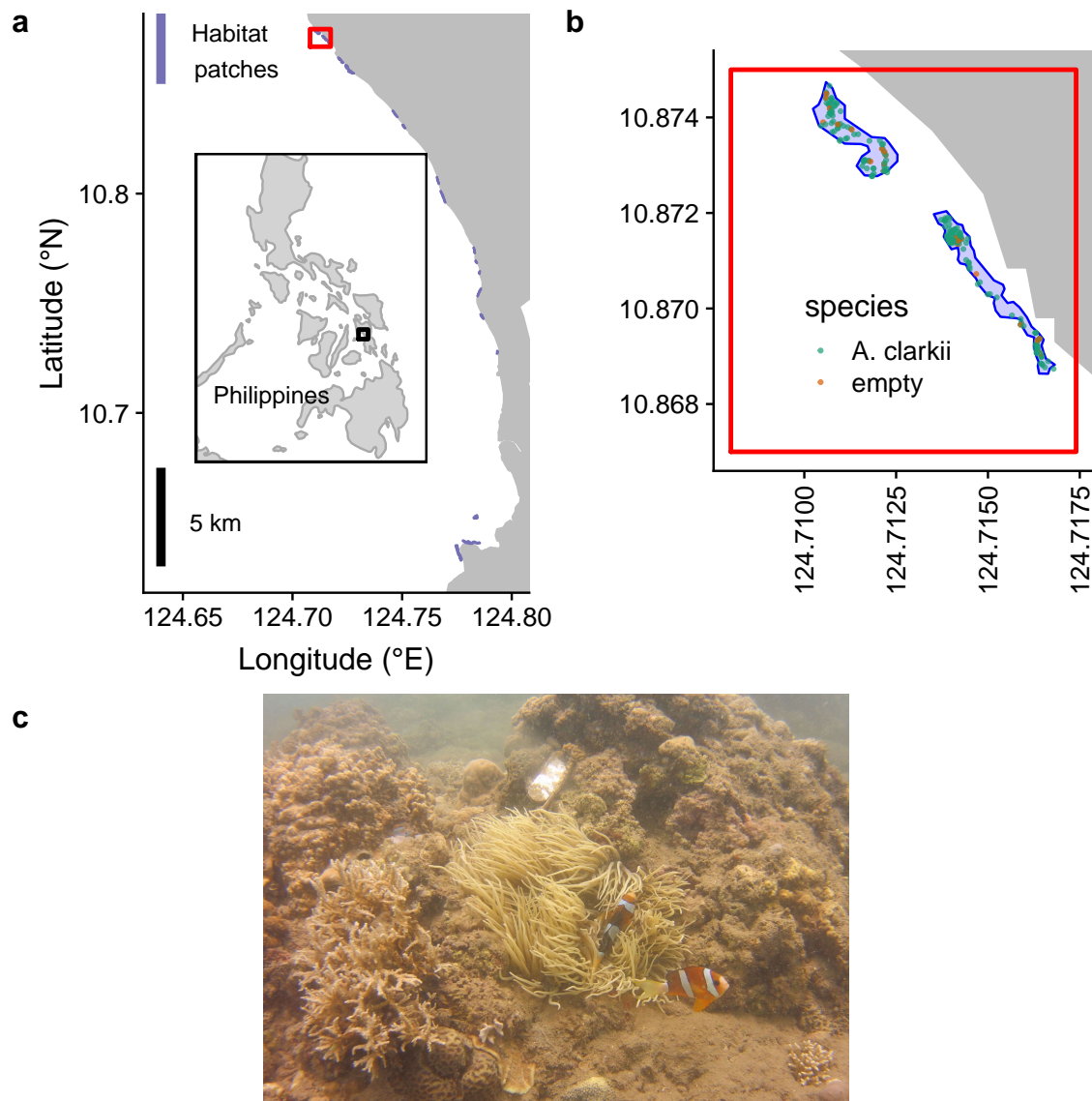


Figure 3: a) Map of the sites along the coast of Leyte in the Philippines. b) Zoomed-in map of the two northern-most sites, Palanas and Wangag, to show anemone arrangement, with anemones occupied by *A. clarkii* (green) or unoccupied by clownfish (orange). c) An example anemone occupied by *A. clarkii* in a typical habitat at the sites. The metal anemone tag is visible just above the anemone on the rock.

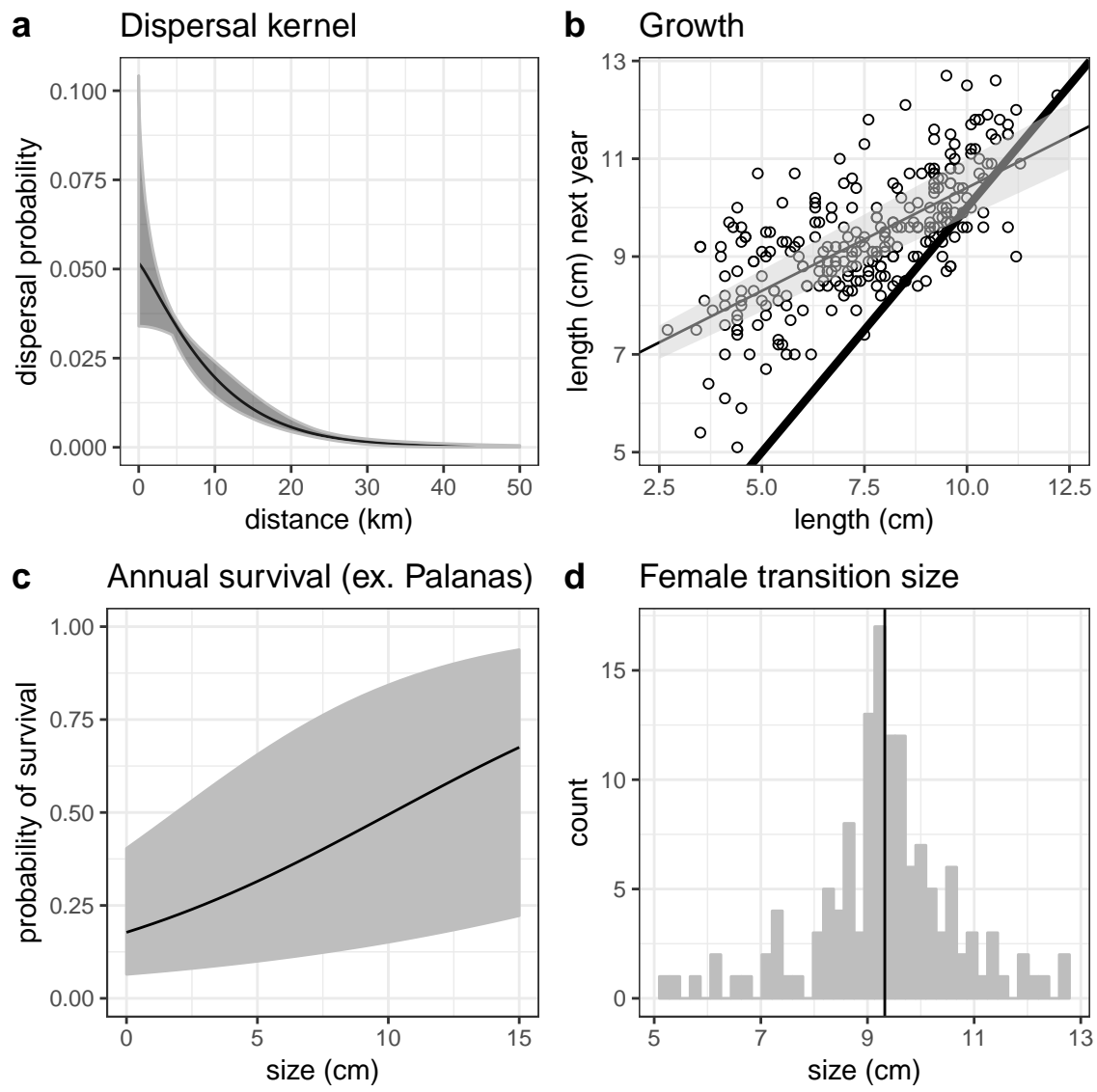


Figure 4: Best estimates (solid black line) and range included for uncertainty (gray) for dispersal (a), growth, including the 1:1 line in thick black (b), post-recruit survival at Palanas as an example site (c), and size at female transition (d) parameters.

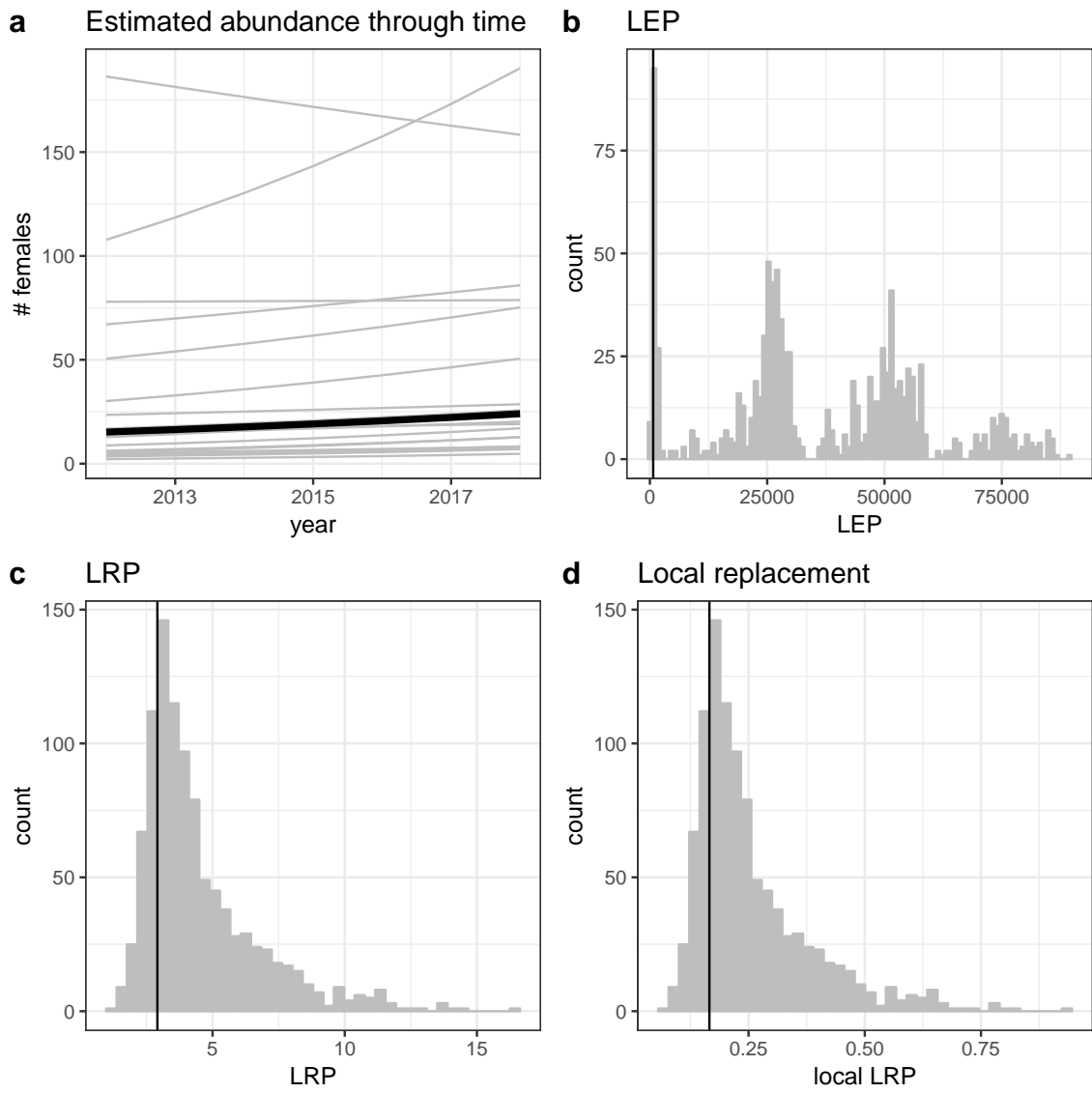


Figure 5: Estimates of a) estimated abundance of females at each site (grey lines) and for an average site (black line) b) average LEP across sites, c) LRP, and d)  $LRP_{local}$ , showing the best estimate (black solid line) and range of estimates considering uncertainty in the inputs. The estimates in c-d include our attempt to remove density-dependence in the early life stages. We only consider density-dependence in egg-recruit survival so LEP (a) estimates are the same in both cases.

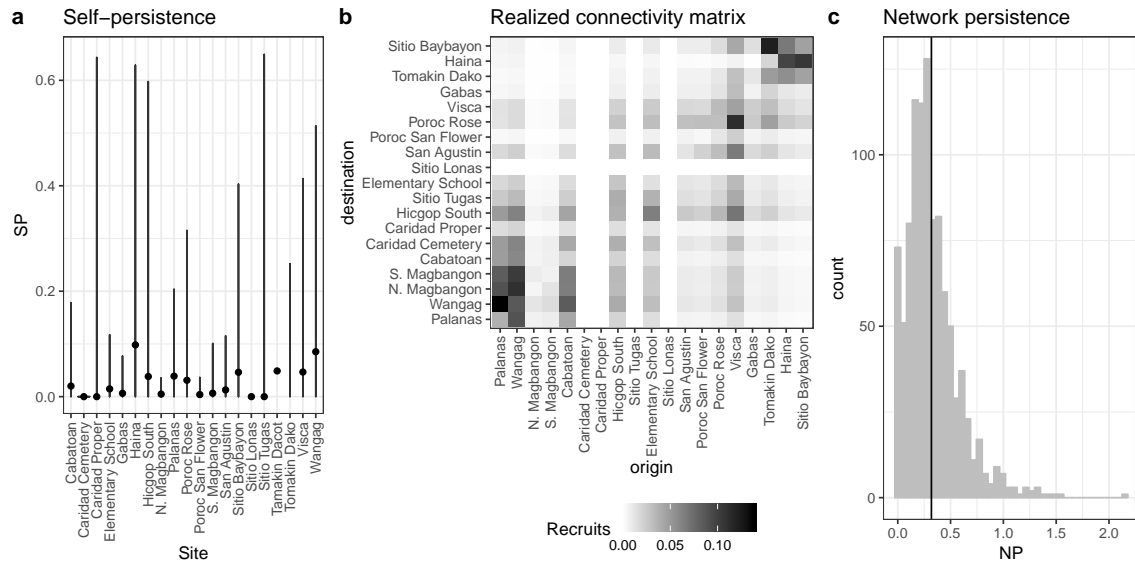


Figure 6: Values of self-persistence (a), realized connectivity among sites (b), and network persistence (c). All estimates include compensation for density-dependence in early life stages in our data. For self-persistence (a) and network persistence (c), the best estimate is shown with in black (point for (a), line for (c)) and the range of estimates considering uncertainty is shown in grey.

# Appendix

## Summary of parameters

Parameter	Description	Best estimate	Range in uncertainty runs	Notes
$k_d$	scale parameter in dispersal kernel	-2.11	-2.36 to -1.96	estimated using methods in Bode et al. (2018) in Catalano et al. (in prep)
$\theta$	shape parameter in dispersal kernel	1	NA	estimated using methods in Bode et al. (2018) in Catalano et al. (in prep)
$L_\infty$	average asymptotic size in von Bertalanffy growth curve	10.70 cm	10.50 to 10.90 cm	

$K$	growth coefficient in von Bertalanffy growth curve	0.864	0.785 to 0.944	
$b_\phi$	intercept for adult survival	-1.82	$\pm 0.231$ standard error	on a log-odds scale
$b_a$	size effect for adult survival	0.169	$\pm 0.028$ standard error	on a log-odds scale
$b_{pr}$	intercept for recapture probability from mark-recapture analysis	2.10	$\pm 0.849$ standard error	on a log-odds scale, not used in persistence estimates
$b_1$	size effect for recapture	-0.161	$\pm 0.088$ standard error	on a log-odds scale, not used in persistence estimates
$b_2$	distance effect for recapture	-0.196	$\pm 0.023$ standard error	on a log-odds scale, not used in persistence estimates

size <sub>recruit</sub>	size (cm) of recruited offspring	mean of size of offspring in parentage analysis = 4.37 cm	3.5 - 6.0 cm	drawn from uniform distribution across range
size <sub>recruit,sd</sub>	standard deviation of size of a recruit	0.1		used in discretization of IPM for LEP
size <sub>sd</sub>	standard deviation distribution of sizes of a fish in the next year	1.45		used in discretization of IPM for LEP, estimated from range of sizes for fish starting at 7.4-7.6 cm and recaptured a year later
$b_e$	coefficient for eyed eggs	-0.608		Yawdoszyn et al. (in prep)
$b_l$	size effect in eggs-per-clutch relationship	2.39		Yawdoszyn et al. (in prep)
$b$	intercept in eggs-per-clutch relationship	1.17		Yawdoszyn et al. (in prep)

$c_e$	egg clutches per year	11.9		Holtswarth et al. (2017)
$L_f$	size at transition to female	9.32cm	5.2 - 12.7cm	drawn from distribution in data
$P_h$	proportion of sites sampled cumulatively across time	0.41		details in A.1
$P_d$	proportion of dispersal kernel area from each site covered by our sampling region	0.57		details in A.2
$P_c$	probability of capturing a fish	0.56	drawn from beta distribution with parameters $\alpha_{P_c} = 1.44$ and $\beta_{P_c} = 1.13$	details in A.2

$P_s$	proportion of our sampling region that is habitat	0.20		details in A.3
DD	proportion of habitat that would be available without density-dependence at settlement	1.71		
$p_U$	proportion of anemones unoccupied by clownfish	0.53		used to estimate DD
$p_A$	proportion of anemones occupied by <i>A. clarkii</i>	0.38		used to estimate DD

Table A1

528 **A Method details**

### A.1 Proportion of habitat sampled

We used tagged anemones to estimate the proportion of habitat sampled at each site  
531 in each year ( $P_{h_{i,t}}$ ). We tagged each anemone that is home to *A. clarkii*, with a metal tag, which is relatively permanent and easy to re-sight (the anemone tag is visible above the anemone in Fig. 3c), so we consider the total number of metal tags at each site to be the total number of anemones that are habitat. We divide the number of tagged anemones visited each sampling year by the total number of metal tags at that site to get the proportion of habitat sampled. We use proportion of anemones rather than proportion of total site area because anemones, and therefore habitat quality, are unevenly distributed across the site; areas we did not visit are likely to have a lower density of anemones than the areas we did sample.

540 For scaling the number of tagged recruited offspring to account for areas of our sites we did not sample, we use the overall proportion habitat sampled across all sites and sampling years ( $P_h$ ). We sum the metal-tagged anemones we visited across all sites and years to get the total number of metal-tagged anemones we visited while sampling. We then divide that by the number of anemones we could have sampled, the sum of total metal-tagged anemones across all sites multiplied by the number of sampling years, to get the overall proportion habitat sampled across our sites and sampling years.

		% Habitat surveyed						
Site	# Total anems	2012	2013	2014	2015	2016	2017	2018
Cabatoan	26	42	58	58	65	73	0	62
Caridad Cemetery	4	0	75	50	0	50	50	50
Elementary School	8	0	100	38	88	88	88	100
Gabas	9	0	0	0	44	44	67	0
Haina	104	0	6	13	13	10	56	80
Hicgop South	18	0	67	22	28	56	83	78
N. Magbangon	105	5	12	40	63	63	0	5
S. Magbangon	34	41	56	32	0	65	0	71
Palanas	137	29	58	47	63	85	86	86
Poroc Rose	13	100	100	69	31	23	69	69
Poroc San Flower	11	100	82	73	73	55	82	64
San Agustin	17	94	65	71	65	100	82	76
Sitio Baybaon	260	0	14	30	33	30	41	80
Tomakin Dako	50	0	24	22	36	34	60	68
Visca	13	100	100	23	38	62	85	62
Wangag	296	18	32	42	34	26	49	68

Table A2: Table showing the percent of metal-tagged anemones surveyed at each site in each sampling year.

## A.2 Probability of capturing a fish, from recapture dives

549 We use mark-recapture data from recapture dives done within a sampling season to  
estimate the probability of capturing a fish. During some of the sampling years (XX),  
portions of the sites were sampled again XX-XX weeks after the original sampling  
dives. We assume there is no mortality of tagged fish between the original sampling  
dives and the recapture dives because they are so close in time and that fish do not  
change their behavior or response to divers, so therefore assume that the probability  
555 of recapturing a fish is the same as the probability of capturing a fish on a sample dive.  
For each recapture dive, we use GPS tracks of the divers to identify the anemones  
covered in the recapture dive and the set of PIT-tagged fish encountered on those  
558 anemones during the original sampling dives. We estimate the probability of capture  
 $P_c$  as the number of tagged fish caught during the capture dive  $m_2$  divided by the  
total number of fish caught on the recapture dive  $n_2$ :  $P_c = \frac{m_2}{n_2}$ .

561 We use the mean  $P_c$  across all 14 recapture dives, covering XX sites in 3 sampling  
seasons (2016, 2017, 2018), as our best estimate. Because there are so few recapture  
dives compared to the number of times we calculate the metrics to show the range  
564 of uncertainty, we represent the probability of capture as a distribution, rather than  
pulling directly from the values calculated for each recapture dive. The distribution  
of capture probabilities across the 14 dives is quite skewed so we represent it as a  
567 beta distribution, using the mean  $\mu_{P_c}$  and variance  $V_{P_c}$  of the set of 14 values to find  
the appropriate  $\alpha_{P_c}$  and  $\beta_{P_c}$  parameters, where

$$\alpha_{P_c} = \left( \frac{1 - \mu_{P_c}}{V_{P_c}} - \frac{1}{\mu_{P_c}} \right) \mu_{P_c}^2 \quad (\text{A.1})$$

$$\beta_{P_c} = \alpha_{\mu_{P_c}} \times \frac{1}{\mu_{P_c} - 1}. \quad (\text{A.2})$$

The mean of the individual capture probability values is  $\mu_{P_c} = 0.56$ , with variance  
 570  $V_{P_c} = 0.069$ , which gives beta distribution parameters  $\alpha_{P_c} = 1.44$  and  $\beta_{P_c} = 1.13$ .  
 We sample 1000 values from the beta distribution, then truncate the sample to only  
 values larger than the lowest value of  $P_c$  estimated in an individual dive (0.20), to  
 573 avoid extremely low values that are sometimes sampled but are unrealistically low.  
 We then sample with replacement from the truncated set to get a vector of values  
 the length of the number of runs.

## 576 Proportion of dispersal kernel area sampled

[Add in description of calculation and equation]

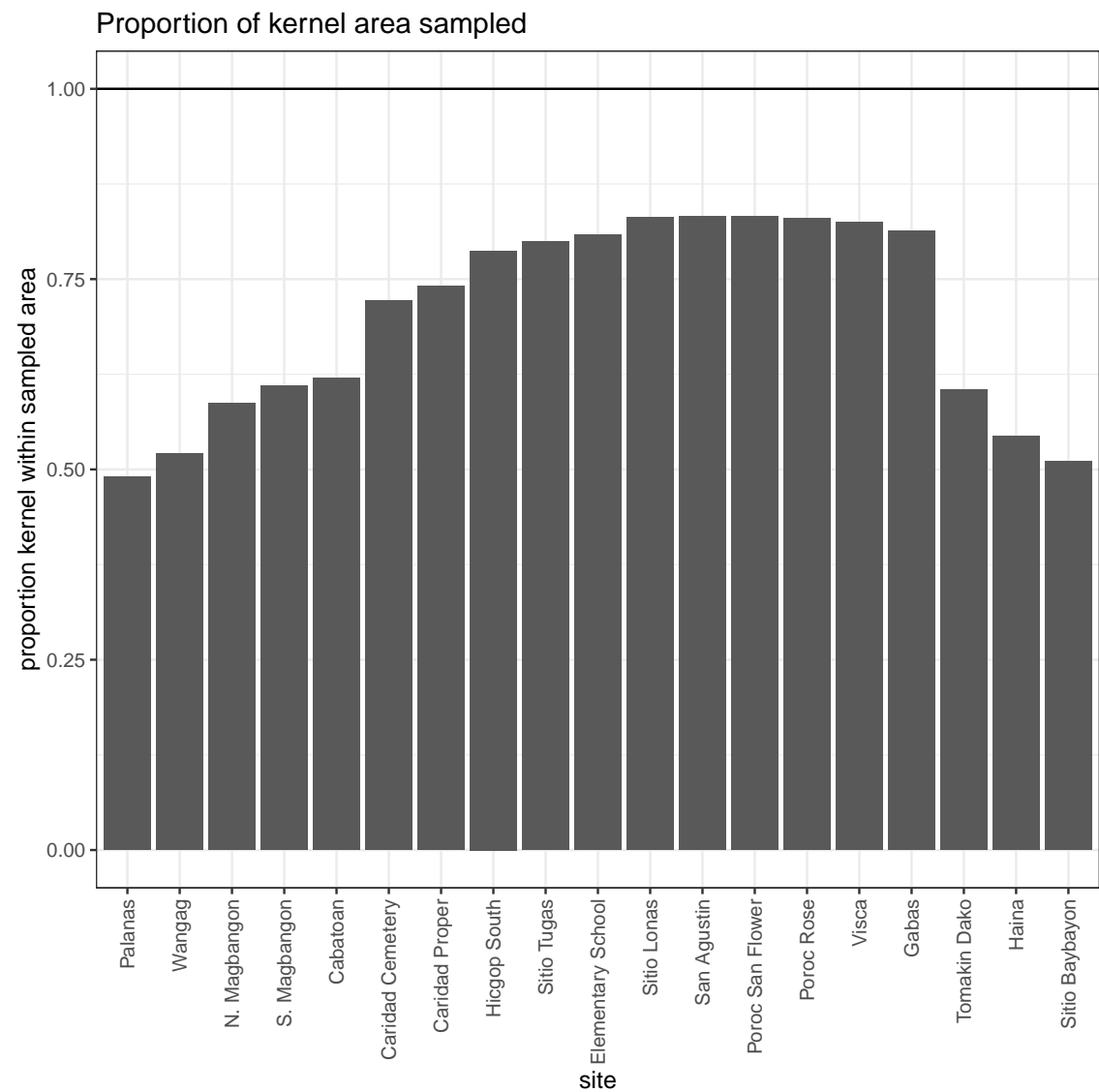


Figure A.1: Proportion of the dispersal kernel area from the center of each site covered by our sampling.

### A.3 Proportion habitat in sampling area

579 We assume that larvae are unable to navigate to habitat if they attempt to settle  
on an unsuitable patch, though clownfish larvae do likely have some ability both to  
sense habitat (CITATIONS) and move toward it (CITATIONS)). To avoid counting  
582 mortality due to settling on non-habitat twice - once in scaling up our matched  
recruits, which only includes those who settled on habitat, and once in integrating  
the dispersal kernel, we scale our estimate of total surviving recruits from our patches  
585 by the proportion of our sampling region that is habitat ( $P_s$ ). We find  $P_s$  by summing  
the lengths of all of our sites, which run approximately north-south, and dividing  
that by the total distance north-south of our sampling region, giving  $P_s = 0.20$ .

Model	Model description	AICc	dAICc
$\phi \sim S, p \sim S + D$	survival size, recapture size+distance	3348.861	0
$\phi \sim S, p \sim D$	survival size, recapture distance	3359.998	-11.1371
$\phi, p \sim D$	survival constant, recapture distance	3383.175	34.3141
$\phi, p \sim S + D$	survival constant, recapture size+distance	3384.959	36.0981
$\phi \sim t, p$	survival time, recapture constant	3408.342	59.4816
$\phi \sim i, p$	survival site, recapture constant	3440.842	91.98112
$\phi \sim i, p \sim S + D$	survival site, recapture size+distance	3440.842	91.98112
$\phi, p \sim t$	survival constant, recapture time	3453.609	104.74839
$\phi \sim S, p \sim S$	survival size, recapture size	3527.710	178.84940
$\phi, p$	survival constant, recapture constant	3570.908	222.04690

Table A3

588 **A.4 Full set of MARK models**

We consider the following set of models in MARK for survival ( $\phi$ ) and recapture ( $p$ ) probability, including effects of size ( $S$ ), minimum distance from diver to anemone 591 during surveys ( $D$ ), time ( $t$ ), and site ( $i$ ) (Table A3):

The best model includes both site and size in survival

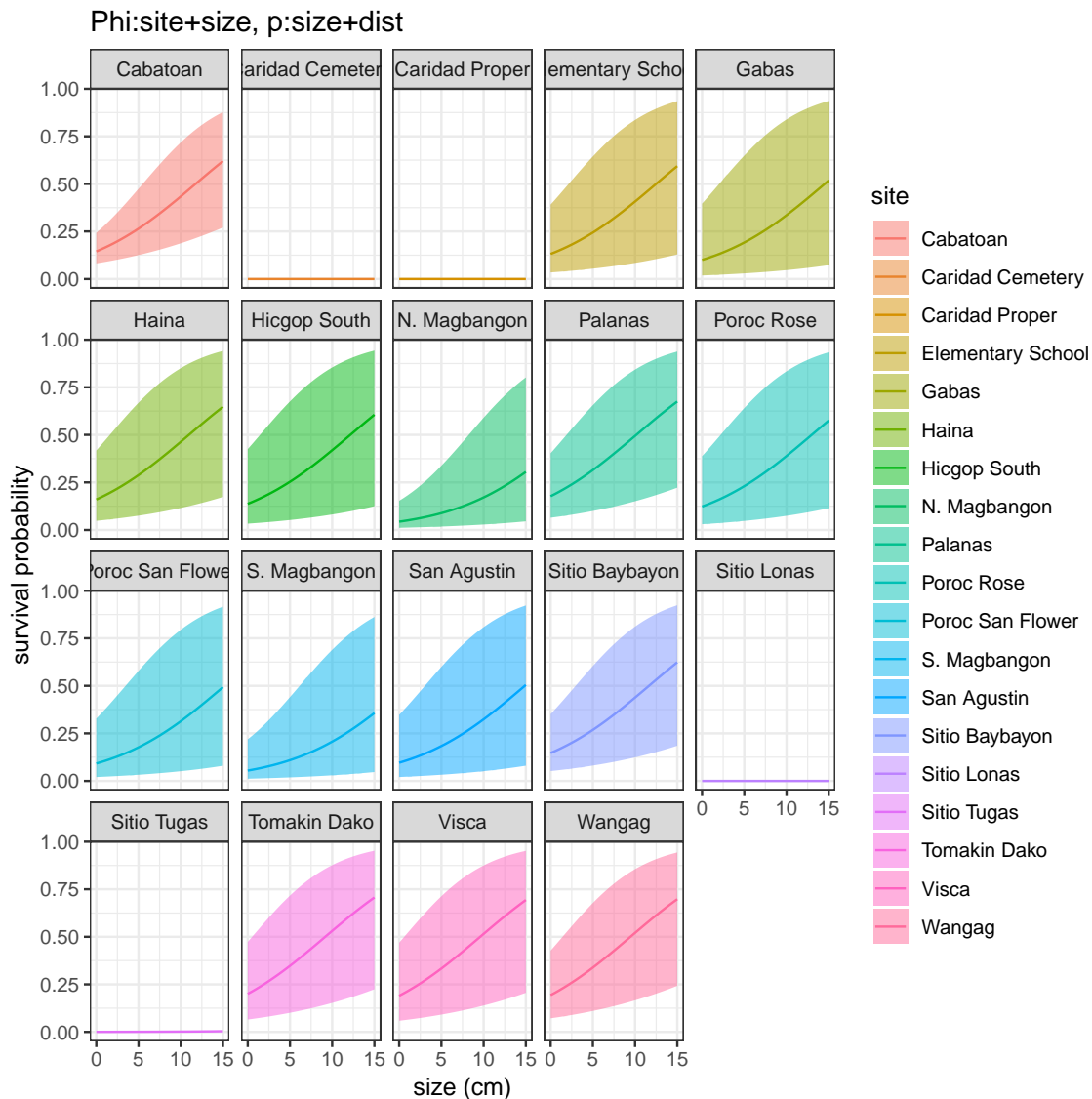


Figure A.2: Annual survival by size at each site.

#### A.4.0.1 Recapture model

<sup>594</sup> The best model for log-odds recapture probability, accompanying the survival model in eqn. 11, has a size effect ( $b_1 = -1.816 \pm 0.080$  SE, Fig. A.3a) and a negative

effect of diver distance from the anemone ( $b_2 = -0.171 \pm 0.021$  SE, Fig. A.3b), with  
597 intercept  $b_{pr} = 17.93 \pm 0.858$  SE:

$$\log\left(\frac{p_r}{1 - p_r}\right) = b_{pr} + b_1 \text{size} + b_2 d. \quad (\text{A.3})$$

The negative effect of both size and distance suggest that divers are less likely to recapture larger fish and those at anemones far from areas sampled.

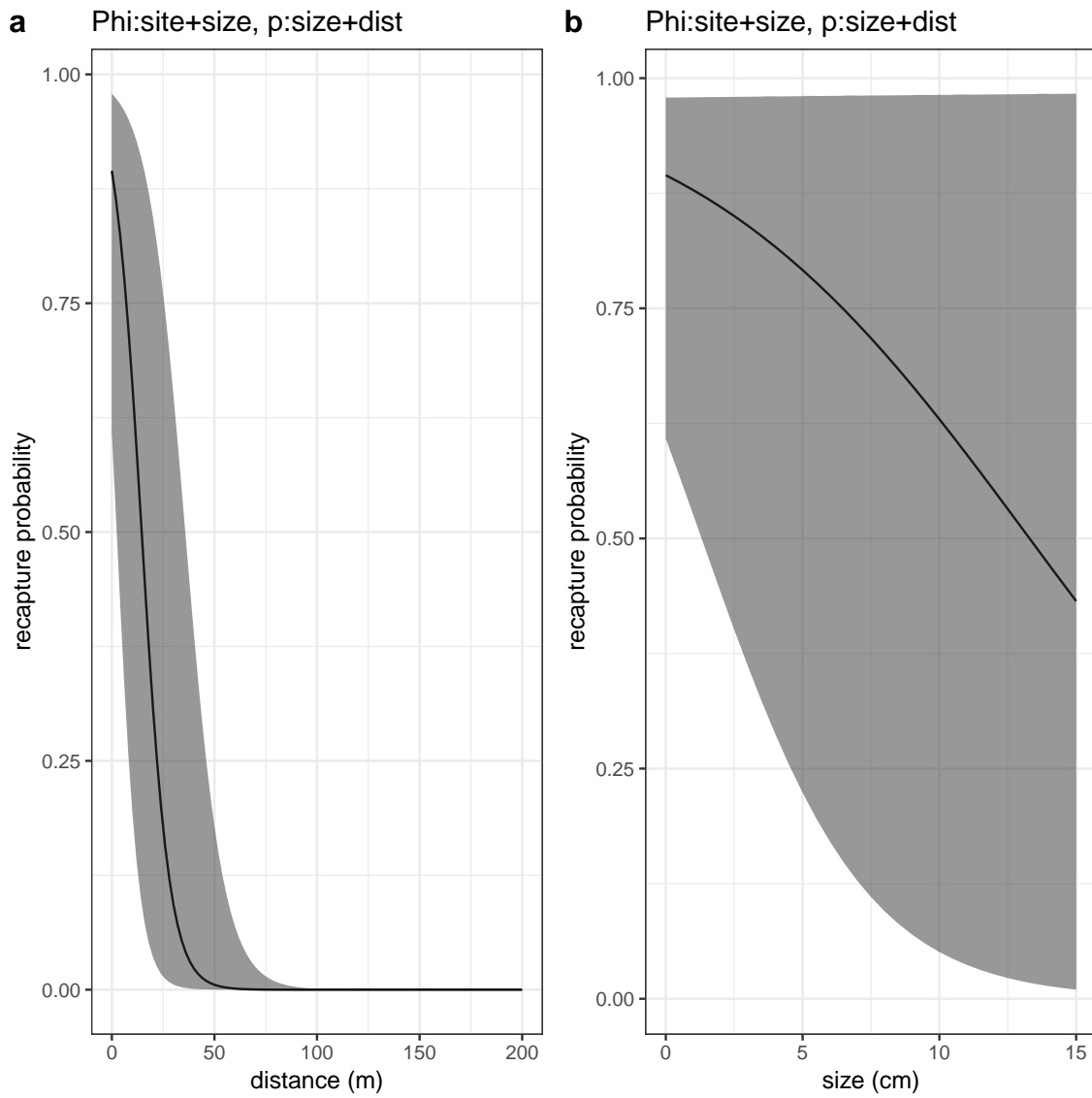


Figure A.3: Effects of a) minimum distance between divers and the anemone where the fish was first caught and b) fish size on the probability the fish will be recaptured, estimated along with survival in a mark-recapture analysis. Size has a slightly negative effect on the probability of recapture - larger fish are stronger swimmers and more likely to flee the anemone when divers approach, but with high uncertainty at larger sizes. Distance also has a negative effect on recapture, as fish tend to stay close to their anemones and are not likely to be recaptured if divers do not get close to their anemone.

## B Result details and sensitivity

### Abundance trends by site

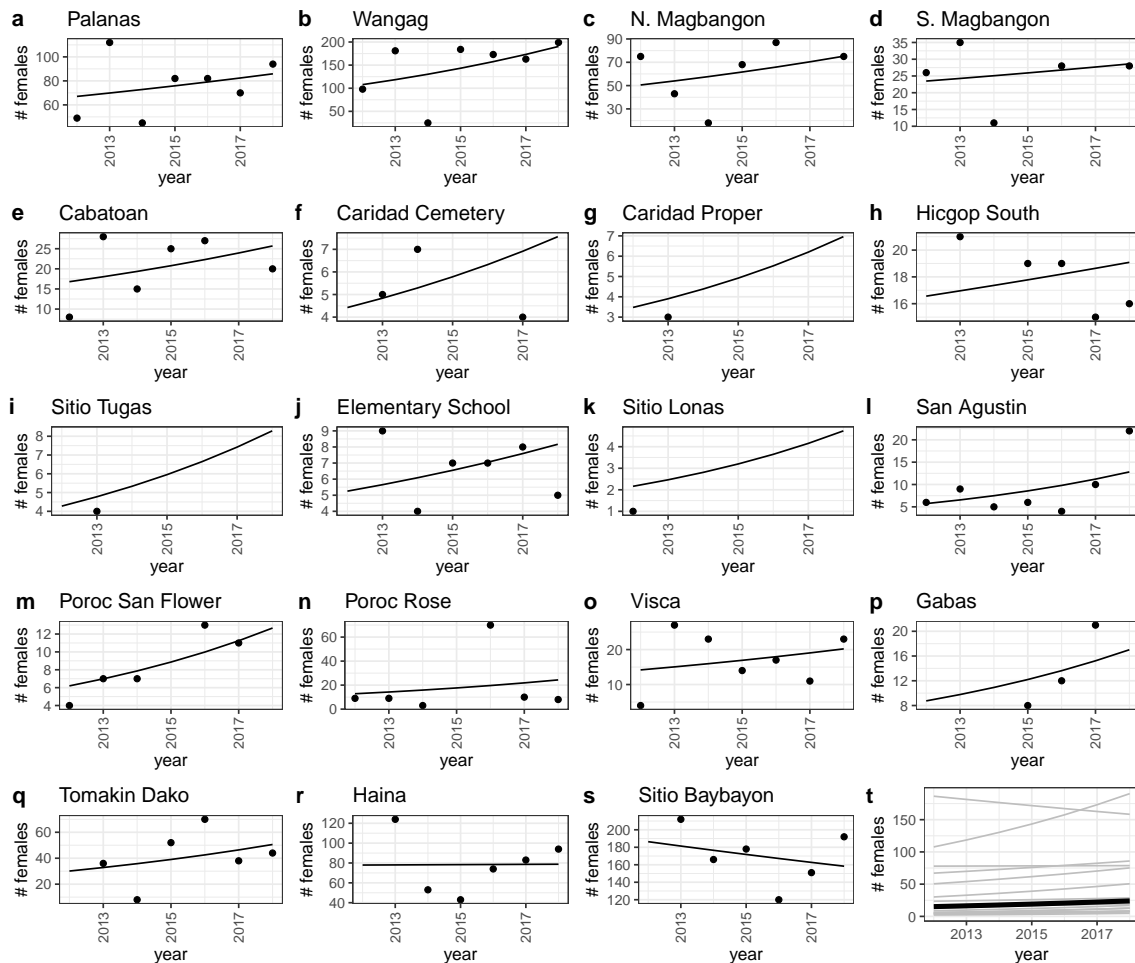


Figure B.1: Scaled estimates of females and abundance trends by site.

## B.1 Sensitivity to parameters

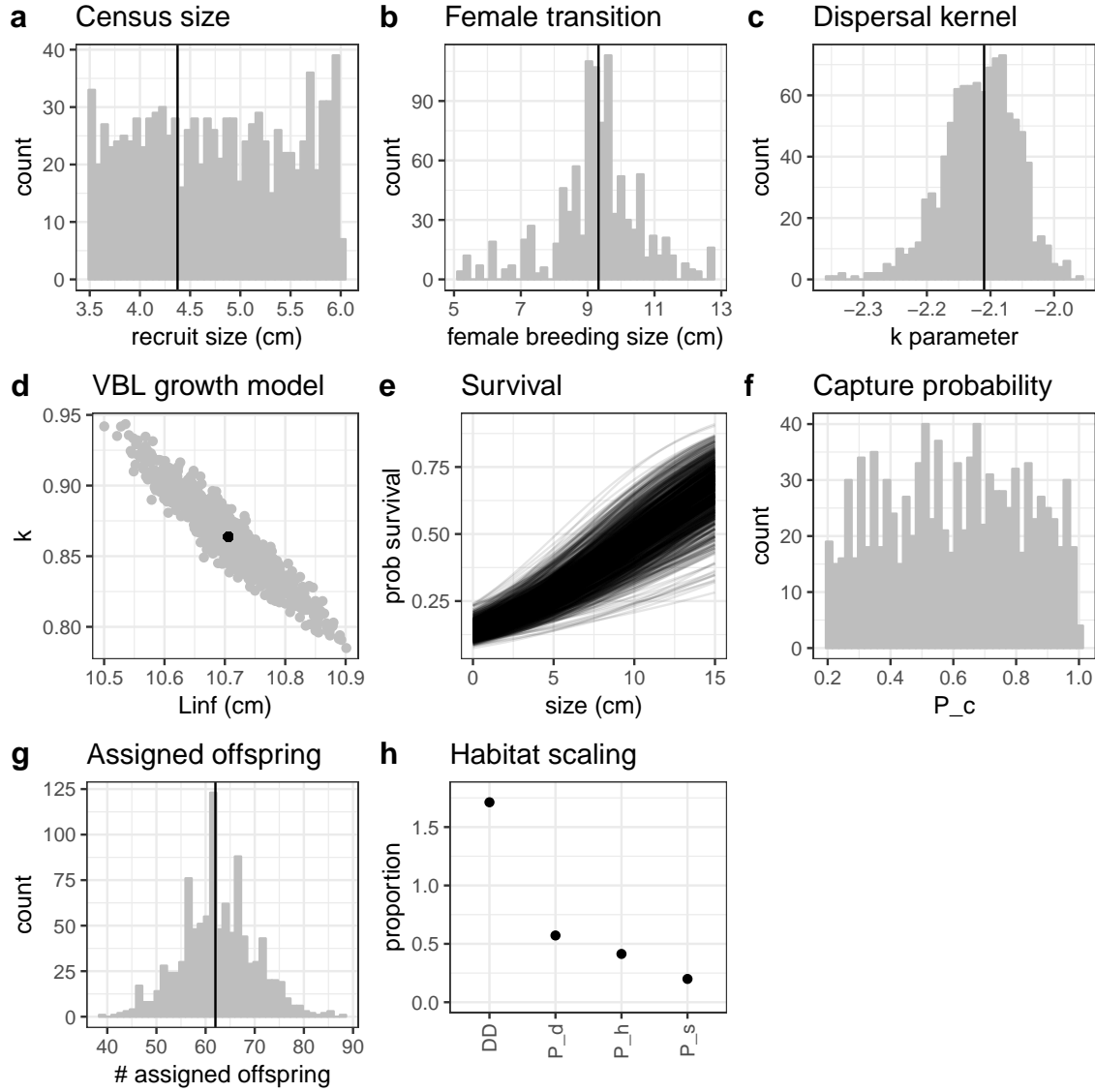


Figure B.2: Range of parameter inputs for uncertainty runs with all uncertainty included: a)  $\text{size}_{\text{recruit}}$ , the census size at which fish are considered to have recruited after egg-recruit survival occurs; b)  $L_f$ , the size at which fish transition from male to female and their reproductive output is included in the estimate of lifetime egg production (LEP); c)  $k_d$ , the scale parameter in the dispersal kernel; d) the parameters  $L_{\infty}$  and  $K$  of the von Bertalanffy growth model; e) the intercept  $b_{\phi}$  of the adult size-dependent survival relationship; f)  $P_c$ , the probability of capturing a fish; g) number of offspring assigned back to parents in the parentage analysis; h) factors that scale the number of estimated recruits from our site based on density-dependence in settler success (DD), proportion of the dispersal kernel captured by our sampling region ( $P_d$ ), the cumulative proportion of our sites we sampled over time ( $P_h$ ), and the proportion of our sampling area that is habitat ( $P_s$ ).

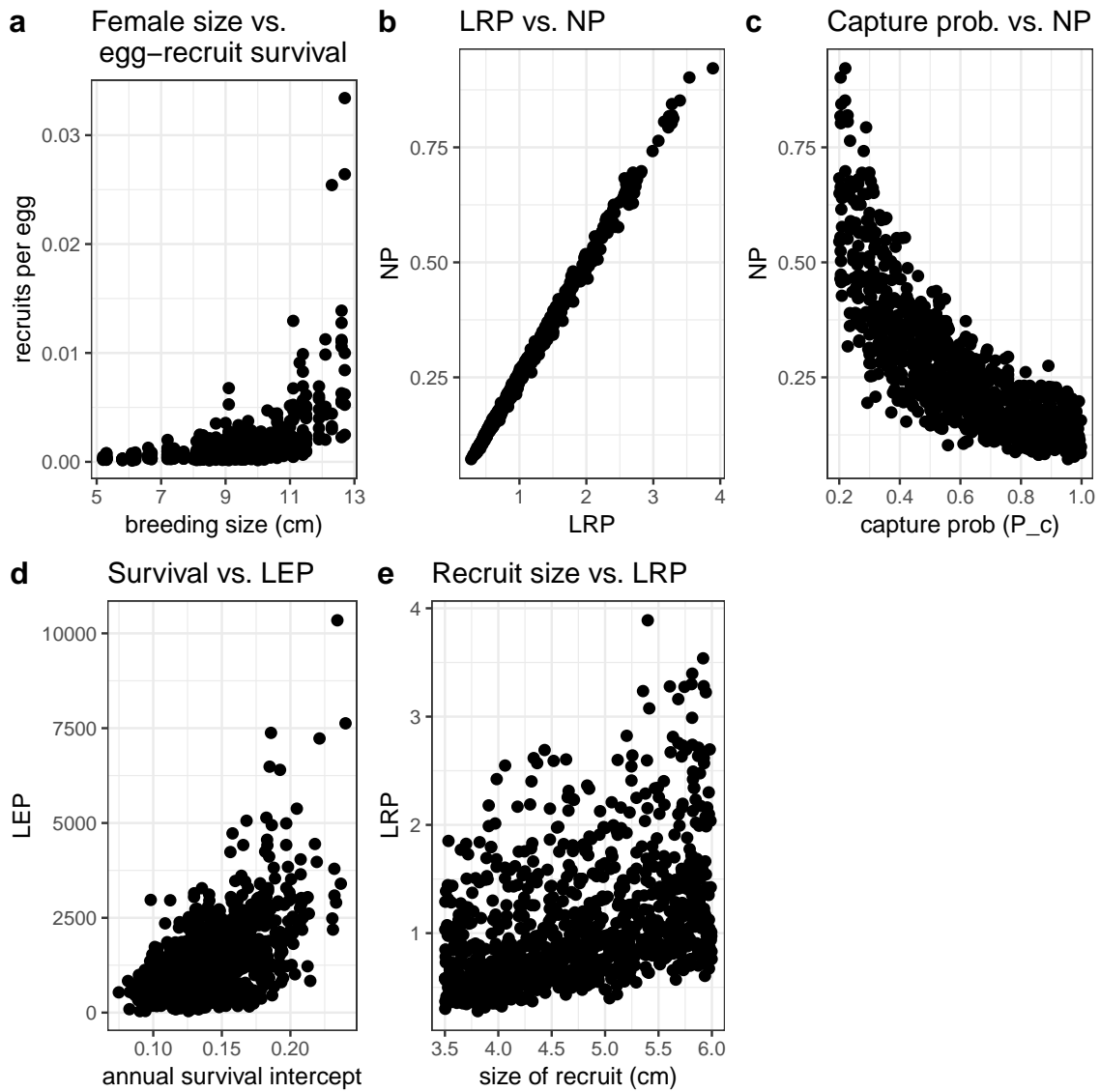


Figure B.3: Relationships among parameters and metrics. a) We only count reproductive effort by fish in the female stage so the higher the transition size to breeding female, the fewer eggs parents are considered to produce, which increases the estimated egg-recruit survival. b) LRP strongly affects NP by changing the number of potential recruits dispersed through the connectivity matrix. c) The probability of capturing a fish does not have a clear relationship to NP. d) LEP is higher with higher survival estimates because fish are more likely to survive longer as reproducing adults. e) The size we consider to be a recruit marks the transition of mortality included in egg-recruit survival to mortality being captured by annual adult survival. Because we do not have the data to change egg-recruit survival to account for different recruit sizes, increasing the recruit size increases LRP by wrapping more mortality into the egg-recruit survival estimate, rather than LEP.

603 **B.2 Effects of different types of uncertainty on metrics**

**B.2.0.1 Lifetime egg production (LEP)**

Annual survival post-recruitment provides drives most of the uncertainty in LEP,  
606 as lower survivals keep fish from reaching and staying at large breeding sizes, with  
higher fecundity. The transition size to breeding female also drives uncertainty in  
LEP - the higher the transition size to female, the less time the fish has at a size  
609 where its reproduction is counted in LEP.

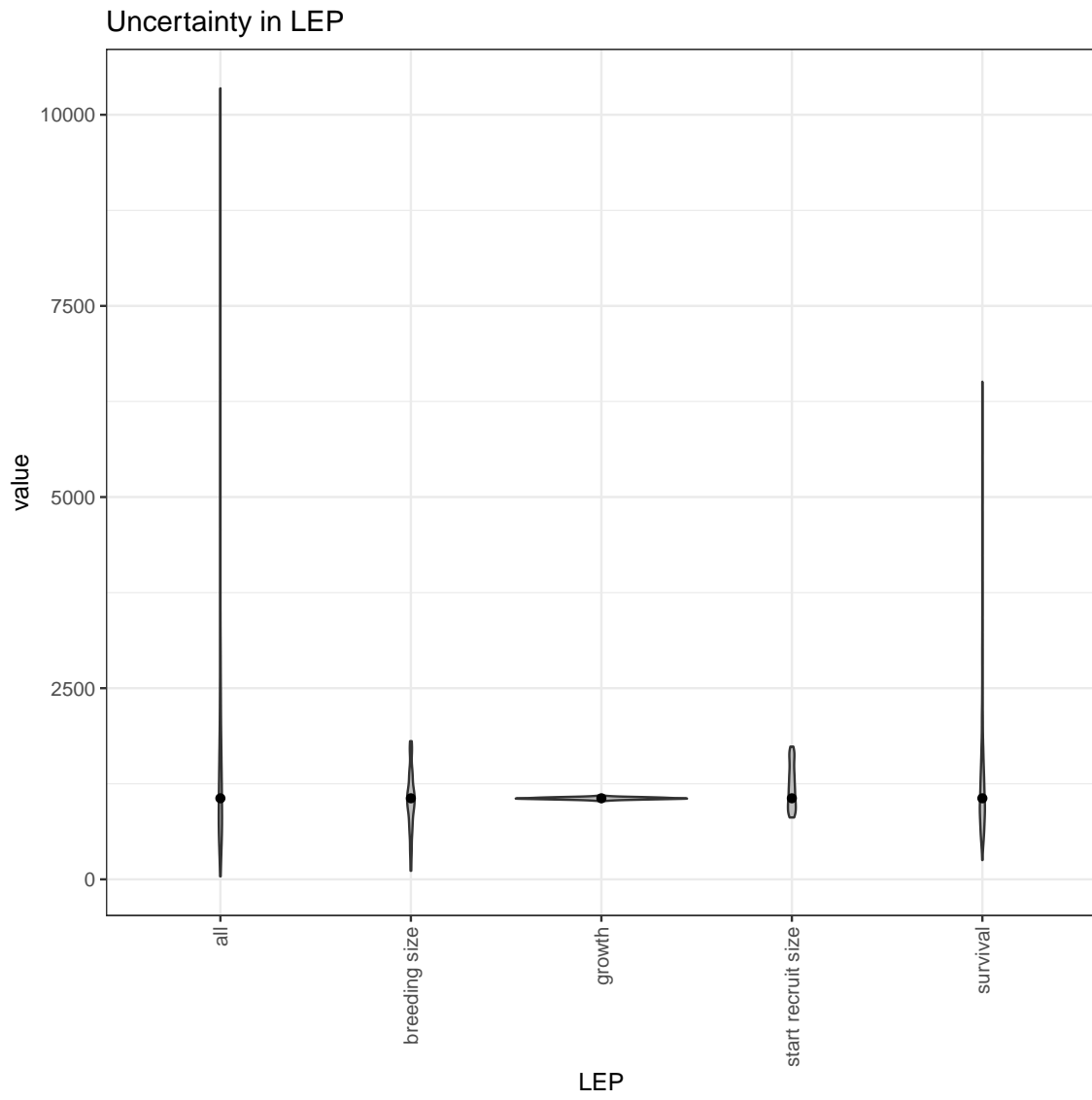


Figure B.4: The contribution of different sources of uncertainty in LEP.

### B.2.0.2 Lifetime recruit production (LRP)

Most of the uncertainty in LRP comes from uncertainty in the size of a recruit. This  
<sub>612</sub> is an artifact of our sampling, where we are unable to estimate egg-recruit survival

differently to account for changes in the size of a recruit, so raising the size of a recruit reduces the mortality included in LRP without increasing the mortality included in  
615 egg-recruit survival, as it should in an ideal situation.

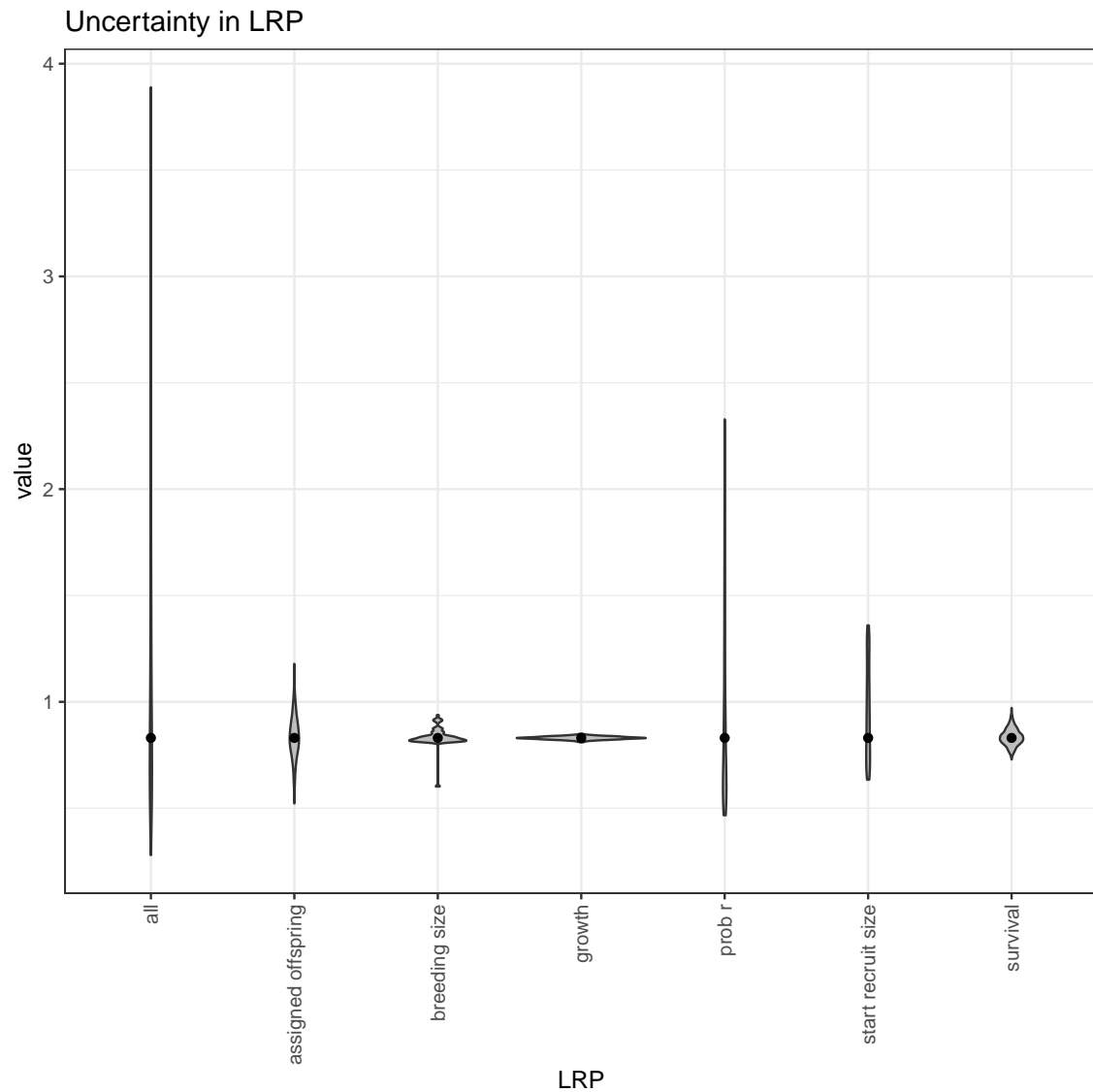


Figure B.5: The contribution of different sources of uncertainty in LRP.

### Uncertainty in LRP accounting for DD

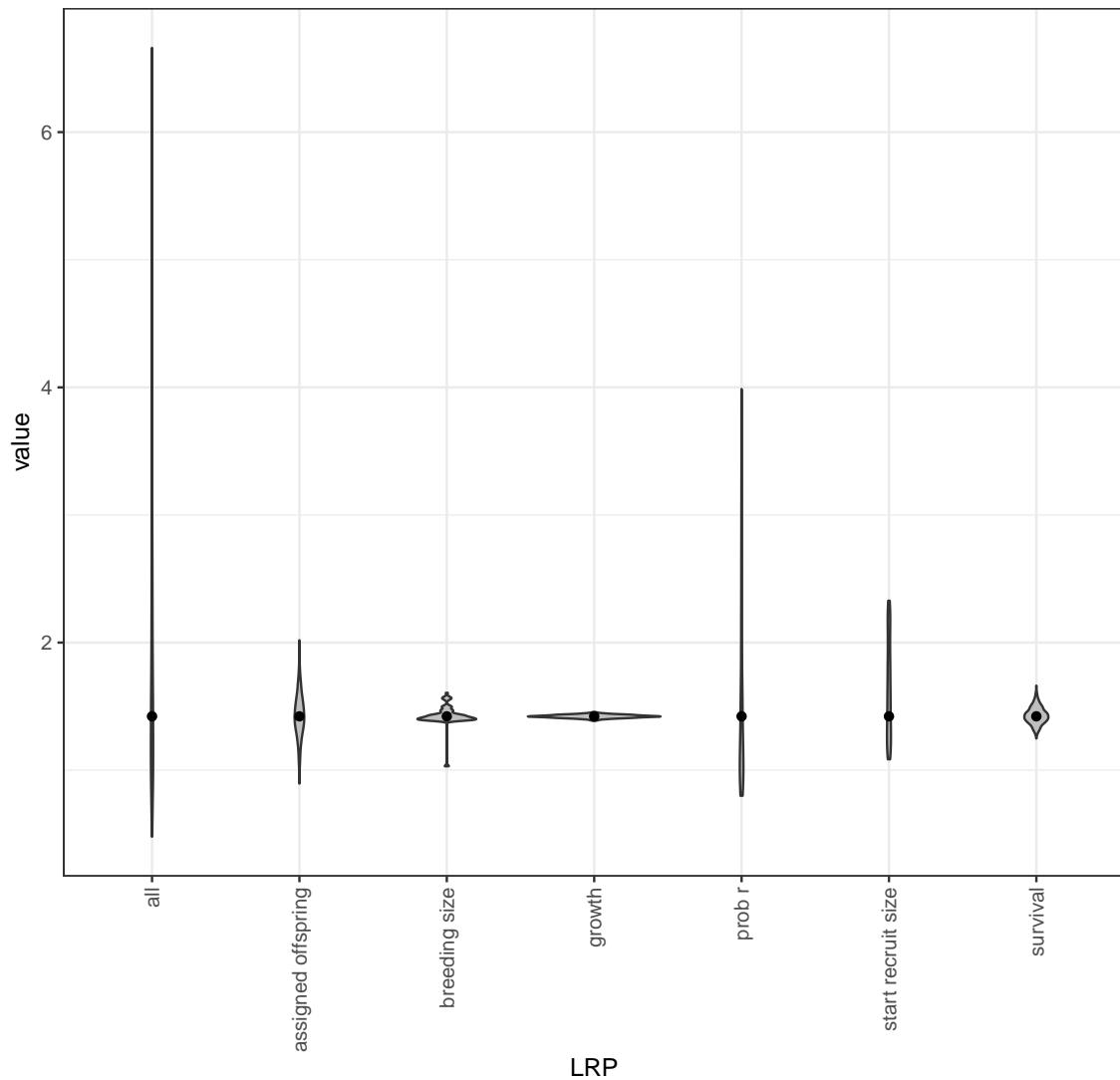


Figure B.6: The contribution of different sources of uncertainty in LRP, when we account for density-dependence in egg-recruit survival.

### B.2.0.3 Egg-recruit survival ( $S_e$ )

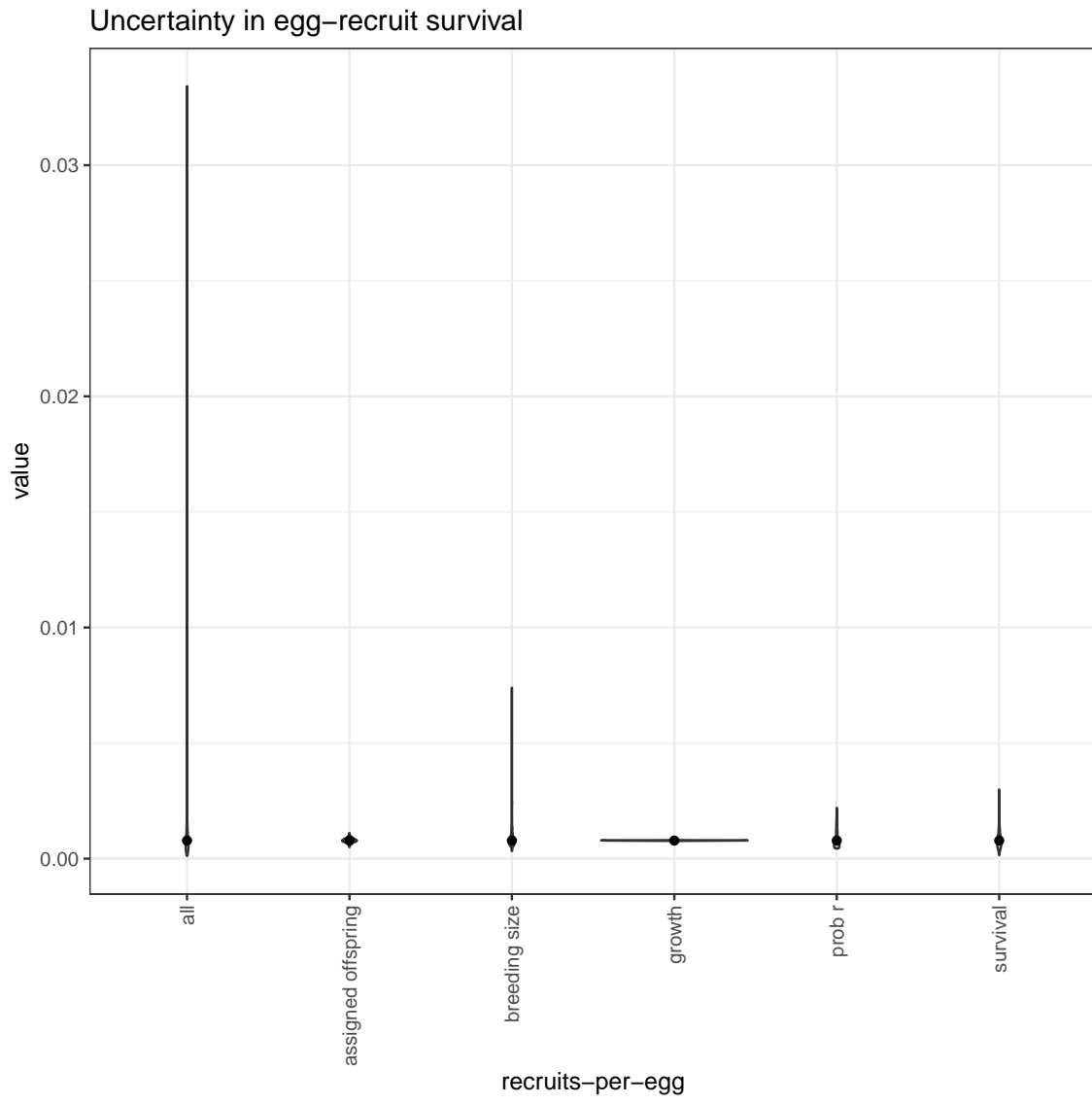


Figure B.7: The contribution of different sources of uncertainty in egg–recruit survival.

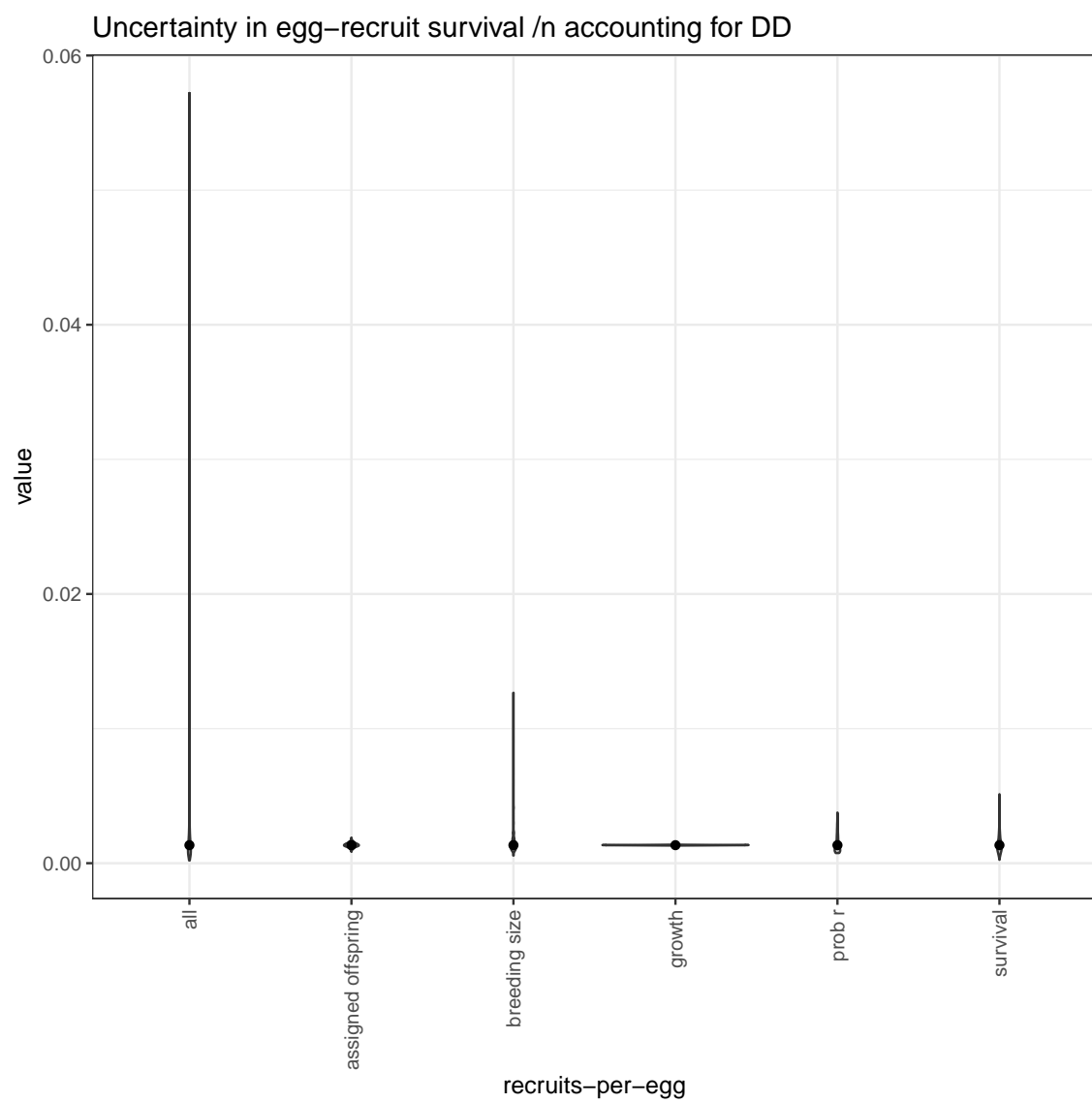


Figure B.8: The contribution of different sources of uncertainty in egg-recruit survival when we account for density-dependence in egg-recruit survival.

#### B.2.0.4 Network persistence (NP)

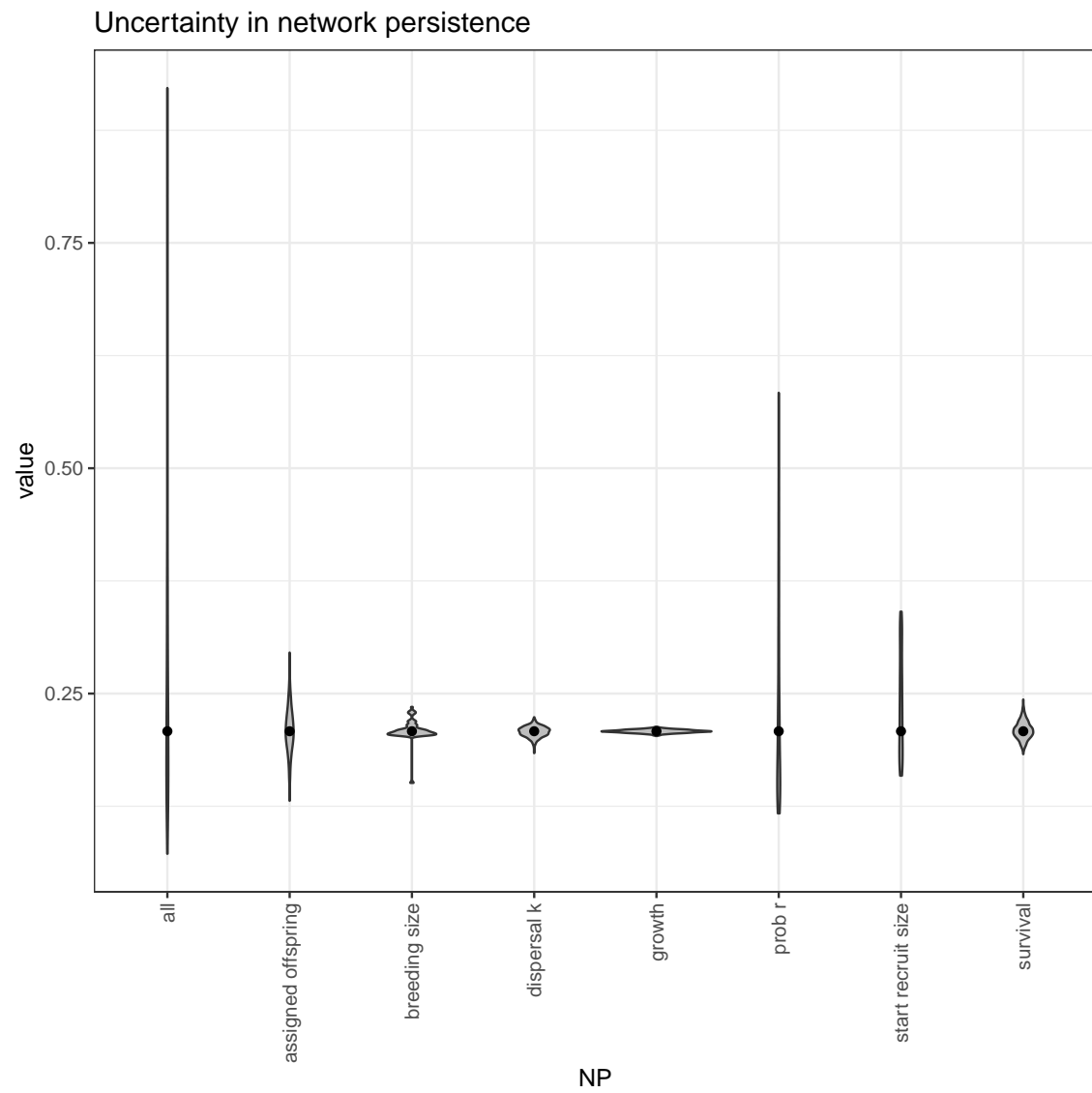


Figure B.9: The contribution of different sources of uncertainty in NP.

### Uncertainty in network persistence /n accounting for DD

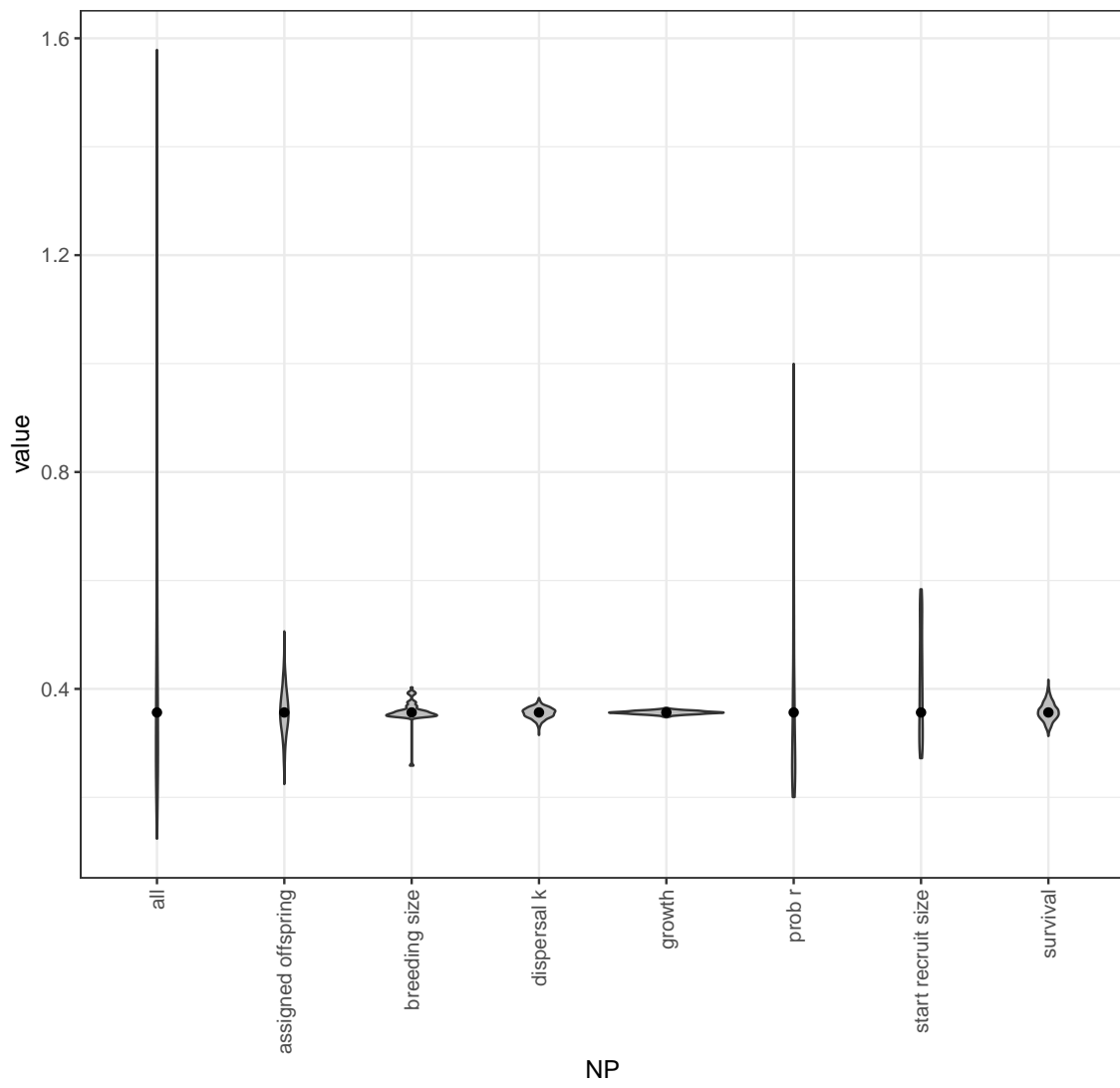


Figure B.10: The contribution of different sources of uncertainty in NP when we account for density-dependence in egg-recruit survival.

## 618 References

- Glenn R Almany, Serge Planes, Simon R Thorrold, Michael L Berumen, Michael Bode, Pablo Saenz-Agudelo, Mary C Bonin, Ashley J Frisch, Hugo B Harrison,  
621 Vanessa Messmer, et al. Larval fish dispersal in a coral-reef seascape. *Nature Ecology & Evolution*, 1:0148, 2017.
- Michael Bode, David H Williamson, Hugo B Harrison, Nick Outram, and Geoffrey P  
624 Jones. Estimating dispersal kernels using genetic parentage data. *Methods in Ecology and Evolution*, 9(3):490–501, 2018.
- L. W. Botsford, J. W. White, M.-A. Coffroth, C. B. Paris, S. Planes, T. L.  
627 Shearer, S. R. Thorrold, and G. P. Jones. Connectivity and resilience of coral reef metapopulations in marine protected areas: matching empirical efforts to predictive needs. *Coral Reefs*, 28(2):327–337, June 2009. ISSN 0722-4028, 1432-  
630 0975. doi: 10.1007/s00338-009-0466-z. URL <http://link.springer.com/10.1007/s00338-009-0466-z>.
- Louis W. Botsford, Alan Hastings, and Steven D. Gaines. Dependence of sustainability on the configuration of marine reserves and larval dispersal distance. *Ecology Letters*, 4:144–150, 2001.  
633
- Scott C Burgess, Kerry J Nickols, Chris D Griesemer, Lewis AK Barnett, Allison G Dedrick, Erin V Satterthwaite, Lauren Yamane, Steven G Morgan, J Wilson White, and Louis W Botsford. Beyond connectivity: how empirical methods can  
636

quantify population persistence to improve marine protected-area design. *Ecological Applications*, 24(2):257–270, 2014.

639

Peter Buston. Forcible eviction and prevention of recruitment in the clown anemonefish. *Behavioral Ecology*, 14(4):576–582, 2003a.

642 Peter Buston. Social hierarchies: size and growth modification in clownfish. *Nature*,

424(6945):145–146, 2003b.

Peter M Buston and Cassidy C DAloia. Marine ecology: reaping the benefits of local

645 dispersal. *Current Biology*, 23(9):R351–R353, 2013.

Peter M Buston and Jane Elith. Determinants of reproductive success in dominant

pairs of clownfish: a boosted regression tree analysis. *Journal of Animal Ecology*,

648 80(3):528–538, 2011.

Peter M Buston, Geoffrey P Jones, Serge Planes, and Simon R Thorrold. Probability

of successful larval dispersal declines fivefold over 1 km in a coral reef fish. *Pro-*

651 *ceedings of the Royal Society of London B: Biological Sciences*, page rspb20112041,

2011.

Henry S Carson, Geoffrey S Cook, Paola C López-Duarte, and Lisa A Levin. Eval-

654 uating the importance of demographic connectivity in a marine metapopulation.

*Ecology*, 92(10):1972–1984, 2011.

Hal Caswell. *Matrix population models: construction, analysis, and interpretation*.

657 Sinauer Associates Inc., Sunderland, Massachusetts, 2nd edition, 2001.

Katrina A Catalano, Allison G Dedrick, Michelle Stuart, Jonathan Purtiz, Humberto Montes, Jr., and Malin Pinsky. Interannual variability of genetic connectivity in  
660 a coral reef fish *Amphiprion clarkii*. in prep.

R. K. Cowen. Scaling of Connectivity in Marine Populations. *Science*, 311(5760):  
522–527, January 2006. ISSN 0036-8075, 1095-9203. doi: 10.1126/science.1122039.  
663 URL <http://www.sciencemag.org/cgi/doi/10.1126/science.1122039>.

Robert K. Cowen and Su Sponaugle. Larval Dispersal and Marine Population Connectivity. *Annual Review of Marine Science*, 1(1):443–466, January 2009. ISSN  
666 1941-1405, 1941-0611. doi: 10.1146/annurev.marine.010908.163757. URL <http://www.annualreviews.org/doi/abs/10.1146/annurev.marine.010908.163757>.

C. C. D'Aloia, S. M. Bogdanowicz, J. E. Majoris, R. G. Harrison, and P. M. Buston.  
669 Self-recruitment in a Caribbean reef fish: a method for approximating dispersal kernels accounting for seascape. *Molecular Ecology*, 22(9):2563–2572, May 2013.  
ISSN 09621083. doi: 10.1111/mec.12274. URL <http://doi.wiley.com/10.1111/mec.12274>.

Cassidy C DAloia, Steven M Bogdanowicz, Robin K Francis, John E Majoris, Richard G Harrison, and Peter M Buston. Patterns, causes, and consequences  
675 of marine larval dispersal. *Proceedings of the National Academy of Sciences*, 112(45):13940–13945, 2015.

Augustus J. Fabens. Properties and fitting of the von bertalanffy growth curve.  
678 *Growth*, 29:265–289, 1965.

Daphne Gail Fautin, Gerald R Allen, Gerald Robert Allen, Australia Naturalist,  
Gerald Robert Allen, and Australie Naturaliste. Field guide to anemonefishes and  
681 their host sea anemones. 1992.

Lysel Garavelli, J Wilson White, Iliana Chollett, and Laurent Marcel Chérubin. Population  
models reveal unexpected patterns of local persistence despite widespread  
684 larval dispersal in a highly exploited species. *Conservation Letters*, 11(5):e12567,  
2018.

Sarah O Hameed, J Wilson White, Seth H Miller, Kerry J Nickols, and Steven G  
687 Morgan. Inverse approach to estimating larval dispersal reveals limited population  
connectivity along 700 km of wave-swept open coast. *Proceedings of the Royal  
Society B: Biological Sciences*, 283(1833):20160370, 2016.

690 Ilkka Hanski. Metapopulation dynamics. *Nature*, 396(6706):41–49, 1998.

Deborah R Hart and Antonie S Chute. Estimating von bertalanffy growth parameters  
from growth increment data using a linear mixed-effects model, with an application  
693 to the sea scallop *placopecten magellanicus*. *ICES Journal of Marine Science*, 66  
(10):2165–2175, 2009.

Alan Hastings and Louis W. Botsford. Persistence of spatial populations depends on  
696 returning home. *Proceedings of the National Academy of Sciences*, 103:6067–6072,  
2006a.

Alan Hastings and Louis W. Botsford. A simple persistence condition for structured  
699 populations. *Ecology Letters*, 9(7):846–852, July 2006b. ISSN 1461-023X, 1461-

0248. doi: 10.1111/j.1461-0248.2006.00940.x. URL <http://doi.wiley.com/10.1111/j.1461-0248.2006.00940.x>.

702 Akihisa Hattori and Yasunobu Yanagisawa. Life-history pathways in relation to gonadal sex differentiation in the anemonefish, *amphiprion clarkii*, in temperate waters of japan. *Environmental Biology of Fishes*, 31(2):139–155, 1991.

705 Kina Hayashi, Katsunori Tachihara, and James Davis Reimer. Low density populations of anemonefish with low replenishment rates on a reef edge with anthropogenic impacts. *Environmental Biology of Fishes*, 102(1):41–54, 2019.

708 J. Derek Hogan, Roger J. Thiessen, Peter F. Sale, and Daniel D. Heath. Local retention, dispersal and fluctuating connectivity among populations of a coral reef fish. *Oecologia*, 168(1):61–71, July 2011. ISSN 0029-8549, 1432-1939.  
711 doi: 10.1007/s00442-011-2058-1. URL <http://link.springer.com/10.1007/s00442-011-2058-1>.

Jordan N. Holtswarth, Shem B. San Jose, Humberto R. Montes Jr., James W. Morley,  
714 and Malin. L Pinsky. The reproductive seasonality and fecundity of yellowtail clownfish (*amphiprion clarkii*) off the philippines. *Bulletin of Marine Science*, 93, 2017.

717 Darren W Johnson, Mark R Christie, Timothy J Pusack, Christopher D Stallings, and Mark A Hixon. Integrating larval connectivity with local demography reveals regional dynamics of a marine metapopulation. *Ecology*, 99(6):1419–1429, 2018.

720 Jacob P Kritzer and Peter F Sale. *Marine metapopulations*. Elsevier Academic Press,  
2006.

J.L. Laake. RMark: An r interface for analysis of capture-recapture data with  
723 MARK. AFSC Processed Rep. 2013-01, Alaska Fish. Sci. Cent., NOAA,  
Natl. Mar. Fish. Serv., Seattle, WA, 2013. URL [http://www.afsc.noaa.gov/  
Publications/ProcRpt/PR2013-01.pdf](http://www.afsc.noaa.gov/Publications/ProcRpt/PR2013-01.pdf).

726 Dale R Lockwood, Alan Hastings, and Louis W Botsford. The effects of dispersal  
patterns on marine reserves: does the tail wag the dog? *Theoretical population  
biology*, 61(3):297–309, 2002.

729 Anna Metaxas and Megan Saunders. Quantifying the "Bio-" Components in Bio-  
physical Models of Larval Transport in Marine Benthic Invertebrates: Advances  
and Pitfalls. *Biological Bulletin*, 216:257–272, 2009.

732 Haruki Ochi. Mating behavior and sex change of the anemonefish, amphiprion clarkii,  
in the temperate waters of southern japan. *Environmental Biology of Fishes*, 26  
(4):257–275, 1989.

735 Malin L Pinsky, Humberto R Montes Jr, and Stephen R Palumbi. Using isolation  
by distance and effective density to estimate dispersal scales in anemonefish. *Evo-  
lution*, 64(9):2688–2700, 2010.

738 Mark Rees, Dylan Z Childs, and Stephen P Ellner. Building integral projection  
models: a user's guide. *Journal of Animal Ecology*, 83(3):528–545, 2014.

- J Roughgarden, S Gaines, and H Possingham. Recruitment dynamics in complex  
741 life cycles. *Science*, 241(4872):1460–1466, September 1988. ISSN 0036-8075, 1095-  
9203. doi: 10.1126/science.11538249. URL <http://www.sciencemag.org/cgi/doi/10.1126/science.11538249>.
- 744 Steven S. Rumrill. Natural mortality of marine invertebrate larvae. *Ophelia*, 32  
(1-2):163–198, October 1990. ISSN 0078-5326. doi: 10.1080/00785236.1990.  
10422030. URL <http://www.tandfonline.com/doi/abs/10.1080/00785236.1990.10422030>.
- 747 Ocane C. Salles, Jeffrey A. Maynard, Marc Joannides, Corentin M. Barbu, Pablo  
Saenz-Agudelo, Glenn R. Almany, Michael L. Berumen, Simon R. Thorrold, Ge-  
offrey P. Jones, and Serge Planes. Coral reef fish populations can persist without  
750 immigration. *Proceedings of the Royal Society B: Biological Sciences*, 282(1819):  
20151311, November 2015. ISSN 0962-8452, 1471-2954. doi: 10.1098/rspb.2015.  
1311. URL <http://rspb.royalsocietypublishing.org/lookup/doi/10.1098/rspb.2015.1311>.
- 753 Michelle Stuart, Katrina Catalano, and Malin Pinsky. Home range in clownfish. in  
prep.
- Jinliang Wang. Sibship reconstruction from genetic data with typing errors. *Genetics*,  
166(4):1963–1979, 2004.
- 759 Jinliang Wang. Computationally efficient sibship and parentage assignment from  
multilocus marker data. *Genetics*, 191(1):183–194, 2012.

Jinliang Wang. Estimation of migration rates from marker-based parentage analysis.

<sup>762</sup> *Molecular ecology*, 23(13):3191–3213, 2014.

J Wilson White, Steven G Morgan, and Jennifer L Fisher. Planktonic larval mortality rates are lower than widely expected. *Ecology*, 95(12):3344–3353, 2014.

<sup>765</sup> Jw White, Lw Botsford, A Hastings, and Jl Largier. Population persistence in marine reserve networks: incorporating spatial heterogeneities in larval dispersal. *Marine Ecology Progress Series*, 398:49–67, January 2010. ISSN 0171-8630, 1616-  
<sup>768</sup> 1599. doi: 10.3354/meps08327. URL <http://www.int-res.com/abstracts/meps/v398/p49-67/>.

Adam Yawdoszyn. Fecundity in clownfish. in prep.